HHS Public Access

Author manuscript

Proteins. Author manuscript; available in PMC 2017 November 01.

Published in final edited form as:

Proteins. 2016 November ; 84(11): 1625–1643. doi:10.1002/prot.25105.

Structural Mutation Analysis of PTEN and its Genotype-Phenotype Correlations in Endometriosis and Cancer

Iris N. Smith and **James M. Briggs**

Department of Biology and Biochemistry, University of Houston, Houston, TX 77204-5001

Abstract

The phosphatase and tensin homolog deleted on chromosome ten (*PTEN*) gene encodes a tumor suppressor phosphatase that has recently been found to be frequently mutated in patients with endometriosis, endometrial cancer and ovarian cancer. Here, we present the first computational analysis of 13 somatic missense *PTEN* mutations associated with these phenotypes. We found that a majority of the mutations are associated in conserved positions within the active site and are clustered within the signature motif, which contain residues that play a crucial role in loop conformation and are essential for catalysis. *In silico* analyses were utilized to identify the putative effects of these mutations. In addition, coarse-grained models of both wild-type (WT) PTEN and mutants were constructed using elastic network models to explore the interplay of the structural and global dynamic effects that the mutations have on the relationship between genotype and phenotype. The effects of the mutations reveal that the local structure and interactions affect polarity, protein structure stability, electrostatic surface potential, and global dynamics of the protein. Our results offer new insight into the role in which *PTEN* missense mutations contribute to the molecular mechanism and genotypic-phenotypic correlation of endometriosis, endometrial cancer and ovarian cancer.

Keywords

PTEN; endometriosis; endometrial cancer; ovarian cancer; genotype-phenotype; protein structure stability; anisotropic network model; global dynamics; mutation

INTRODUCTION

Introduction to PTEN

The phosphatase and tensin homolog deleted on chromosome ten (*PTEN*) tumor suppressor is a phosphatase that antagonizes the phosphotidylinositol 3-kinase (PI3K)/Akt signaling pathway suppressing cell survival and proliferation.[1–4] The *PTEN* gene, located at 10q23.3, encodes a 403-amino acid dual-specificity phosphatase that exerts its function as both a lipid and protein phosphatase (dual-specificity): dephosphorylating both protein tyrosine/serine/

Corresponding Author: jbriggs@uh.edu, Phone: 713-743-8366.

Disclosure statement: The authors have no conflicts of interest to declare.

Ethical compliance statement: The enclosed manuscript is a retrospective case report, which does not require the University of Houston's ethics committee approval.

threonine phosphoproteins and lipid phosphoinositides. However, the PTEN protein is widely known for its role in catalyzing the dephosphorylation of phosphatidylinositol (3,4,5)-triphosphate (PIP_3), an important intracellular second messenger, with greater alacrity, lowering its level within the cell.[5] In fact, the architecture of the active site of PTEN is sufficiently large to accommodate the sugar headgroup of inositol phospholipids as a substrate allowing for catalytic specificity.[6] The crystal structure of PTEN reveals two major domains: a lipid phosphatase domain that contains the catalytic active site and a tightly associated C2 domain, which participates in membrane binding.[6] The wall of the active site pocket is delimited in part by the signature motif P loop ($H^{123}CKAGKGR^{130}$), WPD loop (residues 88–98), and TI loop (residues 160–171) which contain residues that are responsible for catalysis (D92, C124 and R130), the overall positive charge within the active site (H93, K125, K128), mediation of loop motion (H123 and G127), and govern the depth and width of pocket (4-residue insertion: K163, K164, G165 and V166).[6] The tumor suppressor function of PTEN is dependent on its phospholipid phosphatase activity and the loss-of-function of the phosphatase catalytic domain is commonly associated with oncogenic *PTEN* mutations.[6–9] Recently, somatic mutations and deletions of *PTEN* have been reported in many types of sporadic tumors, including endometriosis, endometrial and ovarian cancers,[1,10–20] glioblastomas,[3,4] prostate cancers,[21] and melanomas.[22]

Linking PTEN to endometriosis and cancer

Previous studies have implicated alterations of the *PTEN* gene in endometriosis, endometrial and ovarian cancers.[14–17,20,23,24] The incidence of *PTEN* mutations in endometrium tissue of women diagnosed with endometriosis and endometrial hyperplasia is one of the highest among analyzed tumors and the most commonly mutated gene identified in endometrial cancer.[1,25] In fact, data suggest that *PTEN* is more commonly mutated than any other gene including *K-ras* and *p53*[1,25] in endometrial and ovarian cancers, Recent evidence suggests that endometrial and ovarian carcinomas are frequently found in association with endometriosis, suggesting that they arise through malignant transformation.[14–18,20,26,27] Moreover, research suggests that women with endometriosis may experience elevated risks of a variety of different types of cancer.[26] The inactivation of *PTEN* is an early event in endometrial hyperplasia and the development of endometrial and ovarian cancers.[19,25,28] Thus, mutations and/or complete loss of *PTEN* may contribute to the genesis and development of endometriosis and ultimatetly cancer.

Introduction to Endometriosis and malignant transformation—Endometriosis affects an estimated 176 million women worldwide showing no disparity toward age, ethnicity, or social circumstances.[29] It is defined as the presence of endometrial tissue outside the uterine cavity in various areas throughout the body that develops into nodules, lesions, growths, implants or tumors resulting in severe pelvic pain, severe dysmenorrhea (painful menses), dyspareunia (painful intercourse), chronic fatigue, miscarriages and infertility.[30–33]

Despite over three decades of research and significant understanding of endometriosis, the molecular mechanism and pathogenesis underlying its proliferation remains incompletely understood. Although there is currently no known cure, treatment options are available to

manage symptoms associated with the disease. As symptoms become more severe, quality of life is further reduced. Moreover, women with a history of endometriosis are also at an increased risk for developing cancer.[26,34–36] Studies have long suggested that endometrial carcinoma arises through malignant transformation and is thought to occur in 15–40% of all endometriosis cases.[14,27,34] These data suggest that a greater understanding of the complicated mechanism of endometriosis and malignant transformation will not only illuminate its molecular etiology, but may lead to both therapeutic development and early diagnostic methods.

Insights into the catalytic properties of PTEN provide a platform to analyze the mutations found in endometriosis, endometrial cancer, and ovarian cancer. Recent computational studies on PTEN reveal that missense mutations affect its function and structure.[37,38] Therefore a careful dissection of the effects of putative mutations is pertinent to understanding the molecular mechanism in each of the identified phenotypes.

In this study, thirteen somatic missense mutations were identified from published literature, and further validated in the My Cancer Genome database[39] as well as the Catalog of Somatic Mutations in Cancer (COSMIC) database,[40] thus offering a starting point to explore genotype-phenotype correlations in endometriosis and its malignant transformation to endometrial cancer and ovarian cancer. We propose that the phosphatase domain of PTEN may define a region within the active site wherein a small subset of mutations correlate with severe phenotypes characterized by endometrial cancer and ovarian cancer, and mild phenotypes characterized by endometriosis and endometrial hyperplasia. Our study focuses on understanding the impact that these missense mutations have on the structure of PTEN and on investigating the molecular mechanism of each of the phenotypes.

MATERIALS AND METHODS

Endometriosis and cancer mutations dataset

Somatic missense mutations for endometriosis, endometrial cancer, and ovarian cancer were taken from both the My Cancer Genome[39] and the Catalogue of Somatic Mutations in Cancer (COSMIC) (version 49) databases[40] and a comprehensive literature screening was conducted as listed in Table 1. A cut-off of 13 distinct missense mutations were chosen based on the highest percentage and frequency of the individual mutation somatic mutations found in the endometrium and ovaries as indicated in Table S1 and Figure S1.

Protein structure

The wild-type (WT) structure of human PTEN protein crystallized with tartrate (TLA) (PDB ID 1D5R) was downloaded from the Protein Data Bank (PDB).[41] The tartrate molecule was removed and the calculations were conducted on apo PTEN. The mutant structures were built *in silico* by side chain replacement utilizing the Visual Molecular Dynamics (VMD) Mutator Plugin 1.3[42] starting from the WT PTEN (PDB ID: 1D5R) crystal structure file. Thirteen mutant structure models were generated for each of the phenotype mutations (p.G36E, p.G36R, p.H123Y, p.C124S, p.G129E, p.G129R, p.R130G, p.R130L, p.R130Q, p.R173C, p.R173H, p.V191A, and p.T348I).

Energy Minimization of PTEN mutant structures

Energy minimization was performed on each PTEN mutant structure using GROMACS 4.6.3[43] employing the GROMOS53a6 force field[44] to remove possible steric clashes and minimize forces introduced as a result of the mutation. A series of five overall minimization stages were performed to remove any steric clashes and minimize the forces that were introduced as a result of the mutation that was introduced to the WT structure. Each PTEN mutant was subjected to a step-wise energy minimization using the steepest descent method. Step-wise energy minimization involved 5 steps: in step 1 all protein atoms were restrained, in step 2 protein heavy atoms were restrained, in step 3 all protein atoms were restrained again, in step 4 atoms of the protein main chain were restrained and in step 5, unrestrained energy minimization. Total minimization was carried out until convergence where the maximum atomic force was less than 1000 kJ/mol-nm.

All-atom normal mode analysis

All-atom normal mode analysis (NMA) was conducted on representative molecular dynamics (MD) simulations using GROMCAS 4.6.3[43] with GROMOS53a6 force field[44] on (apo) WT PTEN (PDB ID 1D5R) and mutants as a structural basis. Each system was solvated inside a cubic box of simple point charge (SPC) water[45] with at least 10 Å of water between the protein and edges of the box. All simulations were performed in explicit solvent, with chloride (Cl-) counter ions added to obtain neutrality of the system. Periodic Boundary Conditions and a 2 fs time step were employed for each simulation. Each system contained roughly 75,825 atoms. The Particle Mesh Ewald method[46] was used to treat long-range electrostatic interactions and a cutoff of 9 Å was used for non-bonded interactions. A series of five overall minimization stages were performed on each PTEN model to remove any steric clashes and minimize the forces that were introduced as a result of the mutation that was introduced to the WT structure. Each system was then subjected to a step-wise energy minimization using the steepest descent method. The minimized structures were then slowly heated from 0 to 300 K over 100 ps and equilibrated for an additional 250 ps. The system was heated to 300 K by linearly by increasing the temperature, through velocity rescaling, every 10 ps. The production runs were performed in the NPT (isobaric-isothermal) ensemble at 300 K. Bond lengths were constrained using linear constraint solver (LINCS) algorithm and the van der Waals forces were maintained at 1.4 nm. The Berendsen[47] weak coupling method was employed to maintain constant temperature with a temperature coupling relaxation time of 0.1 ps, a pressure coupling constant of 0.5 ps, and a compressibility of $4.5 \bullet 10^{-5}$. The total simulation time for each model was 200 ns and coordinates were recorded every 1 ps. Normal mode analysis of each system was conducted by performing principal component analysis. Normalizing each eigenvalue of the covariance matrix to its total sum yields the percentage of all movements attributable to the corresponding eigenvector. The largest eigenvalues correspond to the principal component modes that best explain the molecular motions sampled by the all-atom system trajectories. The trajectories and principal component projections were visualized using Visual Molecular Dynamics (VMD) Version 1.9.1.[42]

Sequence Conservation

Multiple sequence alignments (MSA) were constructed utilizing CLUSTALW[48] and manually inspected using Jalview.[49] The protein sequence of PTEN was searched against the UniProt[50,51] sequence database to obtain homologous PTEN proteins sequences.

pKa and electrostatic surface potential calculations

The single-site pKa predictions[52–55] were carried out on WT PTEN (Apo) at pH7 using Chemistry at HARvard Molecular Mechanics (CHARMM),[56] and University of Houston Brownian Dynamics (UHBD).[57] The electrostatic surface potential (ESP) calculations were carried out using Adaptive Poisson-Boltzmann Solver (APBS).[58] ESP calculations were generated for WT PTEN and mutants and visualized using Visual Molecular Dynamics (VMD) Version 1.9.1.[42]

The PTEN PDB entry 1D5R, contains the atomic coordinates of the protein as required for calculation of pKa. The pKa input contained partial atomic charges and atomic radii for each atom, maximal number of iterations [300], ionic strength [150 mM], dielectric constant [solvent 80, protein 20], temperature [298K] and spacing [4: 3.0 45 45 45; 1.2 15 15 15; 0.75 15 15 15; 0.25 20 20 20] in Angstroms.

Protein structure stability and flexibility

I-Mutant 3.0 (http://gpcr2.biocomp.unibo.it/cgi/predictors/I-Mutant3.0/I-Mutant3.0.cgi) is a support vector machine (SVM)-based tool that calculates protein stability changes upon mutation either from sequence or structural information.[59] We utilized the structure-based version of I-Mutant 3.0, which classifies the prediction into one of three classes: neutral mutation ($-0.5 \leq \Delta\Delta G \geq 0.5$ kcal/mol), large decrease (<-0.5 kcal/mol), or large increase (>0.5 kcal/mol).[59] The predicted free energy change $\Delta\Delta G$ is based on the difference between unfolding Gibbs free energy change of mutant and native protein (kcal/mol).[59] **CUPSAT** (http://cupsat.tu-bs.de) is a physiochemical modeling program that utilizes a Boltzmann mean-force potential and torsion angles (phi, psi) to predict $\Delta\Delta G$ values and stability changes.[60] CUPSAT also calculates the overall stability change as well as the adaptation (favorable or unfavorable) of the observed torsion angles (phi, psi) as a result of the mutation. The WT *PTEN* structure file (PDB ID 1D5R) was utilized and the residue name and mutation site were required as input.

To further explore the effects of the mutations on structure stability and dynamics we employed **Elastic Network Contact Model (ENCoM)** (http://bcb.med.usherbrooke.ca/encom),[61,62] that utilizes a novel mixed coarse-grained normal mode method to account for the type and extent of pairwise atomic interactions allowing for the calculation of vibrational entropy differences as a result of mutations.[61,62] ENCoM utilizes a potential function with four terms: (1) covalent bond stretching, (2) angle bending, (3) dihedral torsion and (4) non-bonded interaction while taking into consideration the nature and possible effects that the orientation of the side-chains have on dynamics within the context of normal mode analysis. The WT PTEN structure file (PDB ID 1D5R) was utilized and the residue name and mutation site were required as input.

Anisotropic network - normal mode analysis

The anisotropic network model (ANM), is a coarse-grained model utilized to investigate protein dynamics and vibrational functional motions.[63] Utilizing elastic network methodology (ENM), ANM calculations involved only Cα atoms and employed a uniform spring constant γ with a cut-off distance of 1.5 nm for interacting atoms, such that the overall potential of the system is a sum of harmonic potentials.[64,65] Anisotropic displacements and intrinsic collective motions of WT and mutant PTEN structures were analyzed using ProDy[66] and ANM[63] to obtain the six slowest nontrivial normal modes. Visual Molecular Dynamics (VMD) Version 1.9.1[42,66] was utilized for molecular visualization.

RESULTS

Recent studies have revealed an association between *PTEN* and the development of endometriosis suggesting that frequent *PTEN* mutations may contribute to its genesis and development, pointing to a key role for *PTEN* in the etiology.[18,19] Recent evidence suggests that ovarian endometrial carcinomas are frequently found in association with endometriosis suggesting that they arise through malignant transformation.[14–18,20,26,27] Moreover, research suggests that women with endometriosis may experience elevated risks of various types of cancer.[26] Studies indicate that the loss-of-function mutations in *PTEN* are frequent in human cancer and have been found in patients with endometriosis, endometrial cancer, and ovarian cancer.[14–16,19,23,67–69] In an effort to further understand the possible genotype-phenotype correlation of these mutations, we examined the structural effects and phenotypic consequences of *PTEN* missense mutations to provide insight into their disease mechanisms.

PTEN somatic missense mutations

To investigate the pattern of *PTEN* mutations in each of the phenotypes, we analyzed the prevalence of *PTEN* somatic missense mutations from data presented in literature over the past three decades. The spectrum of their associated phenotypes is shown in Table 1. Using the My Cancer Genome and the Sanger COSMIC databases, *PTEN* was screened and the thirteen mutations were confirmed to be within the highest percentage of somatic mutations found in the endometrium and ovaries (Table S1 and Fig. S1). Using these data we investigated the functional impact of the mutations and whether any correlation exists between *PTEN* genotype and disease phenotype.

Mutation clusters within PTEN

The structure of the PTEN protein reveals a phosphatase domain (residues 1–185) and a C2 domain (residues 186–351), which are both vital for tumor suppressor function. The phosphatase domain contains a tyrosine phosphatase signature motif ($H^{123}CKAGKGR^{130}$) that forms a P loop within the active site pocket. Within this loop, the C124 and R130 residues are essential for catalysis. Knowledge of the catalytic mechanism provides a rational basis for understanding a number of the mutations reported within *PTEN*. Thus, we created a histogram, identifying mutational hotspots within the domain structures of PTEN to further highlight mutations surrounding the active site that may affect catalytic activity and structural stability (Fig. 1). We found the vast majority of mutations localized within the

phosphatase domain, particularly the signature motif, suggesting that phosphatase activity is essential for the physiological function of PTEN in tumor suppression.

Mapping mutations to structure of PTEN

To further examine the local structure and interactions around each mutated residue in both domains of PTEN, these mutations were mapped to the three-dimensional structure of PTEN as shown in Figs. 2A–B. We observed that nine mutations associated with severe phenotypes: six (p.H123Y, p.C124S, p.G129E, p.G129R, p.R130G, and p.R130Q) are clustered within the active site pocket, one (p.G36E) is located near the N-terminus and two (p.R173C and p.R173H) are located at the phosphatase-C2 domain interface. Four of the thirteen mutations (p.G36R, p.R130L, p.V191A, and p.T347I) present mild phenotypes and are scattered throughout both PTEN domains (Figs. 1 and 2A–B). p.R173C is involved in both mild and severe phenotypes: endometrial hyperplasia, endometrial cancer and ovarian cancers, respectively (Table 1). Residues C124 and R130 are affected by missense mutations and play significant roles in catalytic activity and protein function. Most importantly, R130 has mutations (R130G, R130L, and R130Q) implicated in each of the three phenotypes: endometriosis, endometrial cancer, and ovarian cancer (Table 1 and Figs. 2A–B). These three distinct R130 mutations considerably change the size of the respective amino side chains such that the local structure and interactions might be disturbed. Three loops (WPD, P, and TI) that comprise the active site pocket of the phosphatase domain are responsible for the overall positive charge (H93, K125, and K128), catalysis (D92, C124 and R130), mediation of loop motion (H123 and G127) and govern the depth and width of the pocket (K163, K164, G165 and V166) (Fig. 2A).[6] Interestingly, the p.G129E mutation is found in patients with endometrioid tumors with high frequency.[8,33] The position of this residue is located at the bottom of the active site cleft near the TI loop that contributes to the extended active site pocket (Figs. 2A–B). Mutations p.G129E and p.G129R reduce the size of the catalytic pocket, thus hindering accommodation of the bulky phosphoinositol moiety of the substrate PIP_3 (Figs. 2A–B).[6] This mutant likely retains protein tyrosine phosphatase (PTP) activity because the phosphorylated inositol head group requires a larger and shallower pocket.[70] Additionally, the glycine is located in a conserved region and is essential at this position to adopt a backbone conformation needed to accommodate the phosphoinositol moiety and a mutation to glutamic acid thereby reduces the flexibility of the backbone (Fig. 3). Substitution of arginine (p.G129R), which has a larger side chain than glutamic acid, results in complete loss of both protein tyrosine phosphatase and lipid phosphatase activities.[70] It is possible that mutations involving the P, WPD, or TI loops disrupt the size and overall positive charge of the active site pocket, the tumor suppressor function of PTEN, and thus contributes to the development of tumors with a more severe phenotype.[71]

Sequence Conservation

Disease-causing mutations are typically located at conserved positions within a protein family since these residues are usually essential for the structure and/or function of the protein.[72,73] Within PTEN, the P loop is highly conserved between species, whereas the WPD and TI loops are more divergent (Fig. 3). The inter-domain interface residues of the phosphatase domain are second only to the P loop in conservation across species and those of the C2 domain are the best-conserved C2 regions (Fig. 2A).[6] The majority of the somatic

missense mutations investigated in this study are located within a contiguous conserved cluster (Fig. 1) formed around the active site and highly conserved P loop as well as the inter-domain region conferring significant phenotypic changes and can be targeted as potential hot-spot regions for the development of novel therapeutic agents in the treatment of endometriosis, endometrial cancer and ovarian cancer.

Effects of the missense mutations on the structural of PTEN

To understand the structural and phenotypic consequences of the missense mutations in PTEN protein, we utilized a combination of molecular modeling, structural analysis, and bioinformatics methods to analyze the identified mutations. The effects of the mutations reveal that the local structure and interactions affect polarity, protein structure flexibility, and electrostatic surface potential. Structural analysis of p.H123Y, p.C124S, and p.R173H reveal that alterations in the residue size and hydrophobicity disturb the structure and disrupt hydrogen bonding (Figs. 4A–D). The signature motif contained in the loop between pβ5-strand and α4-helix includes two residues H123 and C124 essential for the conformation of the P loop and for catalysis, respectively. The mutation of H123 to tyrosine, causes steric clash with Y76 disrupting the π-π stacking between H123 with Y76 and F37 thus extending the pβ5-strand before the P loop (Fig. 4A). Basic residues H93, K125, K128, surround the catalytic C124 residue and R130, and hydrogen bonds with the side chains R130 and T131 (Fig. 4B). The p.C124S mutation introduces a slightly less hydrophobic side chain disrupting the hydrogen bonding interactions, lowering the pKa (Table 3) and presumably its ability to act as a nucleophile with its known substrate $PI(3,4,5)P_3$. In fact, previous research has shown that p.C124S completely inhibits PTEN's lipid and protein phosphatase activity and was defective in phosphatase activity against $PI(3,4,5)P_3$ and $PI(3,4)P_2$.[74,75] The p.R173H mutation disrupts inter-domain hydrogen bonding with W274 (2.2Å to 3.6Å) and imposes steric clash and side chain distortion with nearby residue V262 (Figs. 4C, D).

Predictions on protein structure stability

Individual missense mutations may destabilize a protein and impact its folding ability. To consider this effect and estimate the level of structural destabilization associated with each missense mutation, we predicted quantitative stability changes utilizing multiple programs that calculate the change of the protein structural stability induced by mutations (ΔΔG). In order to provide points of comparison, we utilized multiple programs such as I-Mutant 3.0,[59] Cologne University Proteins Stability Analysis Tool (CUPSAT),[60] and Elastic Network Contact Model (ENCoM) (Table 3).[61,62]

I-Mutant 3.0 was utilized to calculate protein structure stability changes from the predicted free energy change (ΔΔG) upon mutation as provided from either sequence or structural information.[59] I-Mutant 3.0 predicts each of the thirteen mutations (p.G36R, p.G36E, p.H123Y, p.C124S, p.G129R, p.G129E, p.R130G, p.R130L, p.R130Q, p.R173C, p.R173H, p.V191A, p.T348I) to be destabilizing presenting with negative free energy change (ΔΔG) values −1.30, −0.94, −0.67, −1.12, −1.33, −1.03, −2.15, −0.56, −1.56, −1.57, −1.71, −0.18, and −1.61 kcal/mol, respectively. Eight of these mutations (p.G36R, p.H123Y, p.G129E, p.G129R, p.R130G, p.R173C, p.V191A and p.T348I) are in agreement with experimental data that suggests the loss of lipid phosphatase activity toward PIP_3 as a result of the loss of

stability in the protein. CUPSAT was utilized to predict protein stability changes upon single amino acid point mutation using structural environment-specific atom potentials and torsion angle (phi, psi) potentials. The predicted unfavorable torsion angles for the p.G36E, p.C124S, p.R130G, p.R130Q, p.R173C, p.R173H, p.V191A and p.T348I mutations could be the result of the inability of the torsion angles (phi, psi) to adapt to their new environment which contributes to the higher impact of the atom potentials on stability, thus resulting in a stabilizing mutant. The p.R130G mutation results in both a destabilizing mutation and unfavorable torsion angles due to the greater extent of flexibility forcing the backbone into an incorrect conformation that disturbs the local structure. Interestingly, the effect of these mutations on structural stability and dynamics can be further assessed with ENCoM in Figure 5. We chose ENCoM to predict the effect of mutations as it accounts for side-chain and long-range interactions offering a more realistic representation of intramolecular interactions. The p.R130G/L/Q, and p.R173C/H mutants have an increase in dynamics across the phosphatase-C2 domain interface. It has been previously posited that a majority of mutations within the active site pocket exhibit a loss of phosphatase activity as a result of the p.R173C/H mutations, further implicating this region as a possible mutation-driven allosteric interface. R173 forms a salt-bridge with D324 stabilizing the rich hydrogen bond network within the interface. Mutations located at position 173 results in a loss of charge and involve the destruction of this salt-bridge thus impairing the structural stability within the domain interface contributing to a severe phenotype. This further highlights that the integrity of the interface is important for the overall stability of PTEN and these mutations could disrupt the global dynamics of the protein.

Anisoptropic network model analysis to predict global dynamics

To understand how the intrinsic and global dynamics are impacted by each of the missense mutations on PTEN, elastic network models and normal mode analysis were utilized. To achieve this goal, we utilized the ProDy software package[66] for the construction of anisotropic network[63] coarse-grained models of both WT PTEN and mutants to further explore the interplay of the structural and dynamic effects each of the mutants have on the global dynamics of the tertiary structure. Correlation between collective modes was predicted by the calculation of the anisotropic normal mode (ANM) for each of the WT and mutant models. Lower frequency modes contribute to the covariance and entail the most cooperation and largest amplitude motions. ANM analysis exhibited a high cumulative involvement coefficient for the first 10 slow modes. The mode which emphasizes the contribution of the slowest modes and contributes the most to the overall global motions of each model is mode 2 which has the lowest nonzero “frequency” and involvement coefficient of CI_2=1.00 best describing the conformational changes between the WT and mutant models.

Additionally, though pairwise cross-correlations of the residue fluctuations of the first lowest eignevectors (first three modes) are quite similar, the P loop and WPD loop regions were the most flexible in ANM mode 2 (data not shown). Therefore, of the 10 slowest nontrivial normal modes that were analyzed, ANM mode 2 revealed the greatest differences in the motions of WT and mutant models of PTEN. These ANM 2 modes are found to describe

variations of “hinge-bending” and “zipper-like” global movements, thus characterizing their global conformational changes and cooperative motions relative to their mutation (Fig. 6).

Furthermore, to better discriminate the effects induced by each of the mutations on the protein structure, an all-atom normal mode analysis was conducted by calculating principle component analysis on molecular dynamics trajectory ensembles of the WT and mutant models. The projections of the displacement described by the first principle components on the simulated frames were analyzed. The first principal component of each WT and mutant model collectively account for more than ~40% of the total motion and is therefore a suitable approach to analyze protein dynamics. The introduction of a large charged residue (p.G36E/R) causes both local effects on the N-terminal region and the C2 domain (Figs. 7B–C). The p.H123Y, p.C124S and p.G129E mutations (Fig. 7D–F) significantly affect the principal motions of the TI loop and are somewhat close to the WT fingerprint, whereas the other mutations have well-defined dynamic effects. Additionally, the p.C124S mutation (Figs. 7E) has dramatic effects on the N-terminal region and the catalytic loops as well as the CBR3 loop in the C2 domain indicating this mutation induces long-range perturbations. The p.G129R mutation (Fig. 7G), though somewhat similar to p.G129E, has slightly more fluctuation to its principal motions most particularly in the N-terminal region and CBR3 loop. The p.R130G/L/Q mutations (Figs. 7H–J) significantly alter PTEN dynamics in the surrounding active site as well as long-range perturbations mostly due to the fact that the R130 position is catalytic. Interestingly, p.R173C/H mutations (Figs. 7K,L) affect the principal motions of the P, WPD, and TI loops in the active site, and the inter-domain interface, illustrating long-range perturbations. The p.V191A mutation (Fig. 7M) exhibits dynamic patterns similar to p.C124S and p.R130L indicating that this mutation affects the global dynamics of the TI loop in the active site as well as the CBR3 loop. Lastly, T348I mutation (Fig. 7N) reveals principal motions similar to H123Y indicating that this mutation greatly affects the global dynamics of the P, WPD and TI loops in the active site. Overall, each of the mutation motions captures the differences in the global dynamics induced by the effects of each mutation and reveal unique long-range perturbations within the PTEN protein.

Effects of the missense mutations on ionization states of titratable residues

To understand whether the ionization states of titratable groups are affected by missense mutations, pKa calculations were predicted. pKa predictions provide insight into the local environment of critical residues within the active site where the majority of the mutations are clustered (Table 3). The pKa predictions were performed on the apo form of PTEN using the 1D5R structure without the TLA substrate. Thus the apo conformation exposes the active site and was treated with a high dielectric constant of water. Figure 8 illustrates interactions between WT PTEN ionizable residues and the tartrate molecule within the active site. The pKa can shift depending on the surrounding environment thus affecting protein stability and activity. The pKa of D92 was substantially shifted toward greater acidity due to the formation of hydrogen bonds with H93 and K125, thus stabilizing the deprotonated state. H93 is critical for the affinity of negative substrates thus a moderate shift of 5.93 is critical to maintain the catalytically competent protonation state of the residue. The elevated pKa value of D115 is attributable to hydrogen bond formation with basic residues R130 and

K125, serving as a hydrogen bond acceptor. The pKa of H123 is slightly depressed due to hydrogen bond formation with Y76, and disruption of this hydrogen bonding in the p.H123Y mutation leads to destabilization of the protein (Table 2). C124 exhibits a substantial shift toward greater acidity, which is attributable to the surrounding high density of basic residues H93, K125, K128, and R130 (Fig. 8) indicating that cysteine is stabilized in its thiolate form at physiological pH. A mutation from cysteine to serine would disrupt the electrostatic environment thus further perturbing the pKa.

Effects of the missense mutations on electrostatic surface potential

Electrostatic surface potential calculations were generated for WT PTEN and mutants. As expected WT PTEN (apo) is predicted to have a highly positive electrostatic potential surrounding the active site (Fig. 9). Mutations within the active site: p.H123Y, p.R130G, p.R130Q, and p.R130L reduce positive charge resulting in less favorable electrostatic, binding, and specificity interactions with PIP_3, thus contributing to a severe phenotype. The introduction of a large charged carboxylate side chain for buried mutations: p.G36R, p.G36E, p.G129R, and p.G129E imposes backbone conformational constraints, the inability to facilitate loop movement, and exposure to solvent. More specifically, the p.G129E mutation would thus experience electrostatic repulsion when binding to PIP_3 (Fig. 9). The p.R173C/H mutations replace a large residue (R) with smaller ones (C/H), causing a loss in charge while disrupting the inter-domain hydrogen bond network (Figs. 4C,D, 9).

DISCUSSION

Our study comprises an *in silico* effort in examining 13 somatic missense mutations in PTEN associated with endometriosis, endometrial cancer, and ovarian cancer. Though no single method can predict disease phenotype, utilization of a combination of methods based on protein structure stability, sequence evolutionary information, electrostatic potential, and protein global dynamics were employed in order to increase the predictive accuracy. Our observed predictions correlated with a decrease in protein structure stability in each of the associated mutations. I-Mutant 3.0 predicts all 13 mutations to be destabilizing. ENCoM predicts 6 mutations, (p.R130G/L/Q, p.R173C/H and p.V191A) to be destabilizing. The effect of these mutations on structural stability and dynamics were further assessed in Figures 5–7. Our results indicate that the p.R130G/L/Q and p.R173C/H mutants have an increase in dynamics across the phosphatase-C2 domain interface. We predict that mutations at position 130 that result in a change in polarity or charge would result in a reduction in structural stability thus likely impairing the ability to participate in the catalytic mechanism. It is possible that altering WT interaction of this active site residue would affect PTEN function and thus lead to severe phenotype. The loss of positive charge at the R130 position (Fig.9) as well as interaction with neighboring essential catalytic residues C124 and D92 would disrupt overall function of PTEN. The normal catalytic mechanism involves D92 donating a proton to the bridging oxygen of its substrate PIP_3.[76] Subsequently, R130 binds to the D3-phopsphate of PIP_3 and transfers it to neighboring C124; this interaction is possibly lost due to mutations at position 130.[76] Previous studies indicate that mutations within the active site pocket, in addition to p.R173C/H mutants, exhibit inactivated phosphatase activity,[70,77–79] revealing a possible long-range communication, further

implicating this region as a possible mutation-driven allosteric interface. R173 forms a salt-bridge with D324 stabilizing the rich hydrogen bond network within the interface. We predict that mutations at position 173 that result in a loss of positive charge would invoke the destruction of this salt-bridge thus likely to impair the structural stability within the domain interface leading to a severe phenotype. This further emphasizes that the integrity of the interface is important for the overall stability of PTEN and that these mutations could disrupt the global dynamics of the protein. In CUPSAT, 8 mutations (p.G36R, p.H123Y, p.G129E, p.G129R, p.R130G, p.R173C, p.V191A and p.T348I) are predicted to be destabilizing. This is in agreement with experimental data that suggests the loss of lipid phosphatase activity towards PIP_3 as a result of the loss of stability in the protein. The evolutionary-conservative analysis indicated that the majority of the disease-associated mutations are located in highly conserved parts of the PTEN structure (P loop as well as inter-domain region) (Fig. 3). Our most notable observation was the identification of the inter-domain disruption caused by the mutations at positions 130 and 173 that lead to the most dramatic effect on PTEN long-range communication with the protein and its overall function implicating a rather interesting interplay between these two positions that may be involved in a potential mutation-driven allosteric interface. This provides motivation for future studies to further investigate a network of interactions that contribute to a possible allosteric signal transmission and long-range communication. It is known that PTEN plays a key role as a tumor suppressor protein and is involved in a variety of cellular functions and protein-protein interactions.[80] Therefore, any significant changes in structural stability will thus modify the overall function of the protein having a global impact on various pathways involved in tumor suppression regulation.

A literature search revealed that missense mutations p.C124S, p.G129R, p.R130G/L/Q, and p.R173C/H were implicated in a variety of other human diseases. Mice expressing mutations p.C124S and p.G129E manifested particularly aggressive breast tumors.[77,81] Additionally, mutations at positions 130 and 173 occur at a high frequency in central nervous system tumors.[82] The p.C124S mutation has been previously implicated in Autism Spectrum Disorders, Glioblastoma, and Anaplastic Astrocytoma (a rare brain tumor).[83–86] Johnson and Raines[86] demonstrated that p.C124S devastates catalytic activity thus preventing catalysis with its substrate PIP_3. Our results suggest that the replacement of cysteine with serine would greatly alter the dynamics of the N-terminal region, catalytic loops, as well as the CBR3 loop thus affecting membrane binding, indicating this mutation induces long-range perturbations (Fig. 7). In fact, when this mutant was introduced into cells, phospho-AKT levels remained constant and cells did not undergo G1 arrest or apoptosis.[78] The p.G129R mutation has been reported in association with Glioblastoma.[3,87–89] Our results indicate that the p.G129R mutation introduces a larger, positively charged residue into a highly conserved region that destabilizes the structure and thereby contributes to a more rigid P loop (Fig. 7). The flexibility of the native glycine residue may be necessary for PTEN's function.

Additionally, mutations p.C124S, p.G129E, p.R130G alter the polarity and charge of the active site, leading to structural instability and a catalytically inactive mutant. Interestingly, recent experimental research implicates mutations p.C124S and p.G129E as contributing to a more severe phenotype, providing evidence that these inactive mutants disturb the function

of co-expressed WT protein and perhaps aggravate normal cellular behavior.[90] Conversely, mutants retaining partial loss of function associate more frequently with a milder phenotype,[90] this may also explain the mild phenotype seen in p.G129R as well as in the diverse range in severity of phenotype (from mild to severe) as seen in multiple mutations at one position as in p.G36R/E, p.R130G/L/Q, and p.R173C/H as investigated in this study.

It is important to note that missense mutations at position 130 (p.R130G, p.R130L, p.R130Q) are located within the phosphatase domain of the active site and participate in catalytic activity. Recently, p.R130G was identified as belonging to multivariate PTEN mutations associated with endometrial cancer.[71,91] Additionally, p.R130G, p.R130L and p.R130Q mutations have been previously implicated in Glioblastoma,[92–95] Autism Spectrum Disorder,[79] and Anaplastic Astrocytoma,[87] respectively. Our results demonstrate position 130 to be involved in a potential long-range communication pathway with position 173. Additionally, in comparison to WT PTEN, we observed changes in overall global dynamics due to each of the R130 mutations (Figs. 5–7). In the coarse-grained normal mode analyses, the R130 mutants revealed a “hinge-like” motion compared to the “scissor-like” motion of the WT PTEN (Fig. 6). Whereas in the all-atom normal mode analysis of the principal components on the molecular dynamic ensembles, we see not only local effects on the active site induced by the mutations but also disruption of the inter-domain and long-range perturbations.

Previous studies reveal that the majority of the mutations within the active site pocket exhibit a loss of phosphatase activity in addition to the p.R173C/H mutants located within the inter-domain interface (Table 1). Mutation p.R173C is experimentally predicted to reduce PTEN’s catalytic activity towards PIP_3 substrate[77] and thus its function as well. In many instances mutations affecting catalytic sites or protein interaction sites in general, can be sensitive to residue mutations distant from the active site.[96] Our results predict that both p.R173C and p.R173H destabilize the structure and disrupt the inter-domain interface (Table 2) (Figs. 4C–D, 5–7). These mutations are located within a buried hydrophobic core and a rich hydrogen bond network,[6] given this region is also highly conserved and integral to the hydrogen bond network, it further confirms the extreme importance of this interface for the PTEN function. Mutations at position R173 have been found mutated in a variety of cancers and is recognized as being among one of the eight most frequently mutated residues of PTEN.[6] Moreover, p.R173C and p.R173H are both involved in Glioblastoma[83–85,95,97–102] and Anaplastic Astrocytoma,[83–85,98,101,103–107] respectively. In fact, within the COSMIC database alone, PTEN mutations at positions 130 and 173 are distinctly prevalent in endometrial, ovarian, and central nervous system tumors with a high frequency of position 130 mutations in endometrial and ovarian tumors, whereas only 4% of central nervous system (CNS) tumors also occur at this position. Additionally, 18% of CNS tumors correspond to position 173 with high frequency. We observed that mutations p.R130G/L/Q and p.R173C/H have an increase in dynamics across the phosphatase-C2 domain interface and lead to a more severe phenotype (Figs. 5–7). Moreover, our results indicate that mutations at positions 130 and 173 may trigger certain types of allosteric changes as well as long-range communication effects that contribute to the loss of phosphatase activity toward PIP_3, thus giving rise to a severe phenotype. Further analysis of the catalytic as well as

tumor suppressor functions of mutations at position 173 will aid in understanding the significance of mutational targeting of this position in various cancers.

The missense mutations studied within this work allowed for perturbation of the WT properties of PTEN and provided a unique insight into two molecular mechanisms involving mutations at R130 and R173. Though genotype-phenotype correlations of these mutations are not solely attributable to a destabilization in structure, they are a major causative factor in endometriosis, endometrial cancer, and ovarian cancer as highlighted in this research.

CONCLUSION

Our results are not aimed at predicting the definitive value of the ΔΔG changes for each of the missense mutations but rather to gain insight into the stabilizing or destabilizing effects they have on the overall structure of PTEN. The majority of the somatic missense mutations investigated in this study are located within a contiguous conserved cluster (Fig. 1) formed around the active site and highly conserved P loop as well as the inter-domain region inducing structural instability and thus significant phenotypic changes. The results of our study can be exploited for future mutagenesis studies and as a framework to predict PTEN mutation severity beyond existing algorithms. Ultimately, the primary goal was to investigate the genotype-phenotype relationship for each of the missense mutations presented in order that our results could be utilized to develop a more definitive diagnosis protocol and to this end, develop novel therapeutics for treatment of endometriosis, endometrial cancer, and ovarian cancer.

Additionally, our results provide a platform to further assess experimentally the effects of the mutations on stability of the inter-domain interface. To exploit this approach NMR could be utilized to determine the increase of flexibility of the inter-domain interface due to p.R173C and p.R173H mutations. Additionally, shifts in pKa and hydrogen bond rearrangement at p.R130 mutations could also be tested by means of NMR along with thermal or denaturant unfolding methods.

Supplementary Material

Refer to Web version on PubMed Central for supplementary material.

Acknowledgments

The support of Briggs group members (John W. Craft, Guedmiller S. Oliveira, Sladja Maric, Khushboo Singh, Ben Skidmore and Yanyun Liu) at the University of Houston is greatly appreciated. The HLSAMP-Bridge to Doctorate award and the National Cancer Institute of the National Institutes of Health award number: F31/CA174316. The content is solely the responsibility of the authors and does not necessarily represent the official views of the National Institutes of Health.

REFERENCES

1. Risinger JI, Hayes AK, Berchuck A, Barrett JC. PTEN/MMAC1 mutations in endometrial cancers. Cancer Res. 1997; 57(21):4736–4738. [PubMed: 9354433]
2. Li DM, Sun H. TEP1, encoded by a candidate tumor suppressor locus, is a novel protein tyrosine phosphatase regulated by transforming growth factor beta. Cancer Res. 1997; 57(11):2124–2129. [PubMed: 9187108]

3. Li J, Yen C, Liaw D, Podsypanina K, Bose S, Wang SI, Puc J, Miliaresis C, Rodgers L, McCombie R, Bigner SH, Giovanella BC, Ittmann M, Tycko B, Hibshoosh H, Wigler MH, Parsons R. PTEN, a putative protein tyrosine phosphatase gene mutated in human brain, breast, and prostate cancer. Science. 1997; 275(5308):1943–1947. [PubMed: 9072974]
4. Steck PA, Pershouse MA, Jasser SA, Yung WK, Lin H, Ligon AH, Langford LA, Baumgard ML, Hattier T, Davis T, Frye C, Hu R, Swedlund B, Teng DH, Tavtigian SV. Identification of a candidate tumour suppressor gene, MMAC1, at chromosome 10q23.3 that is mutated in multiple advanced cancers. Nat Genet. 1997; 15(4):356–362. [PubMed: 9090379]
5. Gomperts, BKIM.; Tatham, PER. Signal Transduction. California: Elsevier Academic Press; 2002.
6. Lee JO, Yang H, Georgescu MM, Di Cristofano A, Maehama T, Shi Y, Dixon JE, Pandolfi P, Pavletich NP. Crystal structure of the PTEN tumor suppressor: implications for its phosphoinositide phosphatase activity and membrane association. Cell. 1999; 99(3):323–334. [PubMed: 10555148]
7. Gil A, Andres-Pons A, Pulido R. Nuclear PTEN: a tale of many tails. Cell Death Differ. 2007; 14(3):395–399. [PubMed: 17186024]
8. Myers MP, Stolarov JP, Eng C, Li J, Wang SI, Wigler MH, Parsons R, Tonks NK. P-TEN, the tumor suppressor from human chromosome 10q23, is a dual-specificity phosphatase. Proc Natl Acad Sci U S A. 1997; 94(17):9052–9057. [PubMed: 9256433]
9. Wang X, Jiang X. PTEN: a default gate-keeping tumor suppressor with a versatile tail. Cell Res. 2008; 18(8):807–816. [PubMed: 18626510]
10. Kanamori Y, Kigawa J, Itamochi H, Shimada M, Takahashi M, Kamazawa S, Sato S, Akeshima R, Terakawa N. Correlation between loss of PTEN expression and Akt phosphorylation in endometrial carcinoma. Clin Cancer Res. 2001; 7(4):892–895. [PubMed: 11309338]
11. Kong D, Suzuki A, Zou TT, Sakurada A, Kemp LW, Wakatsuki S, Yokoyama T, Yamakawa H, Furukawa T, Sato M, Ohuchi N, Sato S, Yin J, Wang S, Abraham JM, Souza RF, Smolinski KN, Meltzer SJ, Horii A. PTEN1 is frequently mutated in primary endometrial carcinomas. Nat Genet. 1997; 17(2):143–144. [PubMed: 9326929]
12. Tashiro H, Blazes MS, Wu R, Cho KR, Bose S, Wang SI, Li J, Parsons R, Ellenson LH. Mutations in PTEN are frequent in endometrial carcinoma but rare in other common gynecological malignancies. Cancer Res. 1997; 57(18):3935–3940. [PubMed: 9307275]
13. Stambolic V, Suzuki A, de la Pompa JL, Brothers GM, Mirtsos C, Sasaki T, Ruland J, Penninger JM, Siderovski DP, Mak TW. Negative regulation of PKB/Akt-dependent cell survival by the tumor suppressor PTEN. Cell. 1998; 95(1):29–39. [PubMed: 9778245]
14. Dinulescu DM, Ince TA, Quade BJ, Shafer SA, Crowley D, Jacks T. Role of K-ras and Pten in the development of mouse models of endometriosis and endometrioid ovarian cancer. Nat Med. 2005; 11(1):63–70. [PubMed: 15619626]
15. Castiblanco GA, Pires NY, Wistuba OI, Riquelme SE, Andrade ML, Corvalan RA. Pathogenic role of PTEN tumor suppressor gene in ovarian cancer associated to endometriosis. Rev Med Chil. 2006; 134(3):271–278. [PubMed: 16676097]
16. Mandai M, Yamaguchi K, Matsumura N, Baba T, Konishi I. Ovarian cancer in endometriosis: molecular biology, pathology, and clinical management. Int J Clin Oncol. 2009; 14(5):383–391. [PubMed: 19856044]
17. Martini M, Ciccarone M, Garganese G, Maggiore C, Evangelista A, Rahimi S, Zannoni G, Vittori G, Larocca LM. Possible involvement of hMLH1, p16(INK4a) and PTEN in the malignant transformation of endometriosis. Int J Cancer. 2002; 102(4):398–406. [PubMed: 12402310]
18. Obata K, Morland SJ, Watson RH, Hitchcock A, Chenevix-Trench G, Thomas EJ, Campbell IG. Frequent PTEN/MMAC mutations in endometrioid but not serous or mucinous epithelial ovarian tumors. Cancer Res. 1998; 58(10):2095–2097. [PubMed: 9605750]
19. Sato N, Tsunoda H, Nishida M, Morishita Y, Takimoto Y, Kubo T, Noguchi M. Loss of heterozygosity on 10q23.3 and mutation of the tumor suppressor gene PTEN in benign endometrial cyst of the ovary: possible sequence progression from benign endometrial cyst to endometrioid carcinoma and clear cell carcinoma of the ovary. Cancer Res. 2000; 60(24):7052–7056. [PubMed: 11156411]

20. Willner J, Wurz K, Allison KH, Galic V, Garcia RL, Goff BA, Swisher EM. Alternate molecular genetic pathways in ovarian carcinomas of common histological types. Human pathology. 2007; 38(4):607–613. [PubMed: 17258789]
21. Cairns P, Okami K, Halachmi S, Halachmi N, Esteller M, Herman JG, Jen J, Isaacs WB, Bova GS, Sidransky D. Frequent inactivation of PTEN/MMAC1 in primary prostate cancer. Cancer Res. 1997; 57(22):4997–5000. [PubMed: 9371490]
22. Guldberg P, thor Straten P, Birck A, Ahrenkiel V, Kirkin AF, Zeuthen J. Disruption of the MMAC1/PTEN gene by deletion or mutation is a frequent event in malignant melanoma. Cancer Res. 1997; 57(17):3660–3663. [PubMed: 9288767]
23. Zhang H, Zhao X, Liu S, Li J, Wen Z, Li M. 17betaE2 promotes cell proliferation in endometriosis by decreasing PTEN via NFkappaB-dependent pathway. Mol Cell Endocrinol. 2010; 317(1–2):31–43. [PubMed: 19932734]
24. Ali IU, Schriml LM, Dean M. Mutational spectra of PTEN/MMAC1 gene: a tumor suppressor with lipid phosphatase activity. Journal of the National Cancer Institute. 1999; 91(22):1922–1932. [PubMed: 10564676]
25. Maxwell GL, Risinger JI, Gumbs C, Shaw H, Bentley RC, Barrett JC, Berchuck A, Futreal PA. Mutation of the PTEN tumor suppressor gene in endometrial hyperplasias. Cancer Res. 1998; 58(12):2500–2503. [PubMed: 9635567]
26. Brinton LA, Gridley G, Persson I, Baron J, Bergqvist A. Cancer risk after a hospital discharge diagnosis of endometriosis. Am J Obstet Gynecol. 1997; 176(3):572–579. [PubMed: 9077609]
27. Sampson JA. Metastatic or Embolic Endometriosis, due to the Menstrual Dissemination of Endometrial Tissue into the Venous Circulation. Am J Pathol. 1927; 3(2):93–110. 143. [PubMed: 19969738]
28. Montgomery GW, Nyholt DR, Zhao ZZ, Treloar SA, Painter JN, Missmer SA, Kennedy SH, Zondervan KT. The search for genes contributing to endometriosis risk. Hum Reprod Update. 2008; 14(5):447–457. [PubMed: 18535005]
29. Simoens S, Hummelshoj L, Dunselman G, Brandes I, Dirksen C, D'Hooghe T. Endometriosis cost assessment (the EndoCost study): a cost-of-illness study protocol. Gynecol Obstet Invest. 2011; 71(3):170–176. [PubMed: 21160141]
30. Berkley KJ, Rapkin AJ, Papka RE. The pains of endometriosis. Science. 2005; 308(5728):1587–1589. [PubMed: 15947176]
31. Eskenazi B, Warner ML. Epidemiology of endometriosis. Obstet Gynecol Clin North Am. 1997; 24(2):235–258. [PubMed: 9163765]
32. Giudice LC, Kao LC. Endometriosis. Lancet. 2004; 364(9447):1789–1799. [PubMed: 15541453]
33. Koninckx PR, Meuleman C, Demeyere S, Lesaffre E, Cornillie FJ. Suggestive evidence that pelvic endometriosis is a progressive disease, whereas deeply infiltrating endometriosis is associated with pelvic pain. Fertil Steril. 1991; 55(4):759–765. [PubMed: 2010001]
34. Swiersz LM. Role of endometriosis in cancer and tumor development. Ann N Y Acad Sci. 2002; 955:281–292. discussion 293-285, 396–406. [PubMed: 11949955]
35. Baldi A, Campioni M, Signorile PG. Endometriosis: pathogenesis, diagnosis, therapy and association with cancer (review). Oncol Rep. 2008; 19(4):843–846. [PubMed: 18357365]
36. Vlahos NF, Kalampokas T, Fotiou S. Endometriosis and ovarian cancer: a review. Gynecol Endocrinol. 2010; 26(3):213–219. [PubMed: 19718562]
37. Nassiri IGB, Tavassoli M. Bioinformatics Profiling of Missense Mutations. World Academy of Science, Engineering and Technology. 2009; 52:207–209.
38. Mah SKTSH. Computational Analysis of PTEN Gene Mutation. International Journal on Advanced Science Engineering Information Technology. 2012; 2(5):43–46.
39. Lovly, C.; Sosman, J.; Pao, W. My Cancer Genome, version 1.4.13.2487. 2015. http://www.mycancergenome.org
40. Forbes SA, Bindal N, Bamford S, Cole C, Kok CY, Beare D, Jia M, Shepherd R, Leung K, Menzies A, Teague JW, Campbell PJ, Stratton MR, Futreal PA. COSMIC: mining complete cancer genomes in the Catalogue of Somatic Mutations in Cancer. Nucleic Acids Res. 2011(39(Database issue)):D945–D950.

41. Deshpande N, Addess KJ, Bluhm WF, Merino-Ott JC, Townsend-Merino W, Zhang Q, Knezevich C, Xie L, Chen L, Feng Z, Green RK, Flippen-Anderson JL, Westbrook J, Berman HM, Bourne PE. The RCSB Protein Data Bank: a redesigned query system and relational database based on the mmCIF schema. Nucleic Acids Res. 2005; 33(Database issue):D233–D237. [PubMed: 15608185]
42. Humphrey W, Dalke A, Schulten K. VMD: visual molecular dynamics. J Mol Graph. 1996; 14(1): 33–38. 27–38. [PubMed: 8744570]
43. Van Der Spoel D, Lindahl E, Hess B, Groenhof G, Mark AE, Berendsen HJ. GROMACS: fast, flexible, and free. J Comput Chem. 2005; 26(16):1701–1718. [PubMed: 16211538]
44. Oostenbrink C, Villa A, Mark AE, van Gunsteren WF. A biomolecular force field based on the free enthalpy of hydration and solvation: the GROMOS force-field parameter sets 53A5 and 53A6. J Comput Chem. 2004; 25(13):1656–1676. [PubMed: 15264259]
45. Jorgensen WL, Chandrasekhar J, Madura JD, Impey RW, Klein ML. Comparison of Simple Potential Functions for Simulating Liquid Water. Journal of Chemical Physics. 1983; 79(2):926–935.
46. Essmann UPL, Berkowitz ML, Darden T, Lee H, Pedersen LG. A smooth particle mesh Ewald method. Journal of Chemical Physics. 1995; 103:8577–8593.
47. Berensen HJCPJPM, Van Gunsteren WF, Dinola A, Haak JR. Molecular Dynamics with Coupling to an External Bath. Journal of Chemical Physics. 1984; 81:3684–3690.
48. Thompson JD, Higgins DG, Gibson TJ. CLUSTAL W: improving the sensitivity of progressive multiple sequence alignment through sequence weighting, position-specific gap penalties and weight matrix choice. Nucleic Acids Res. 1994; 22(22):4673–4680. [PubMed: 7984417]
49. Waterhouse AM, Procter JB, Martin DM, Clamp M, Barton GJ. Jalview Version 2--a multiple sequence alignment editor and analysis workbench. Bioinformatics. 2009; 25(9):1189–1191. [PubMed: 19151095]
50. Magrane M, Consortium U. UniProt Knowledgebase: a hub of integrated protein data. Database (Oxford). 2011; 2011:bar009. [PubMed: 21447597]
51. Pundir S, Magrane M, Martin MJ, O'Donovan C, UniProt C. Searching and Navigating UniProt Databases. Curr Protoc Bioinformatics. 2015; 50 1 27 21-10.
52. Blachut-Okrasinska E, Lesyng B, Briggs JM, McCammon JA, Antosiewicz JM. Poisson-Boltzmann model studies of molecular electrostatic properties of the cAMP-dependent protein kinase. European biophysics journal : EBJ. 1999; 28(6):457–467. [PubMed: 10460339]
53. Huyghues-Despointes BM, Thurlkill RL, Daily MD, Schell D, Briggs JM, Antosiewicz JM, Pace CN, Scholtz JM. pK values of histidine residues in ribonuclease Sa: effect of salt and net charge. J Mol Biol. 2003; 325(5):1093–1105. [PubMed: 12527310]
54. Laurents DV, Huyghues-Despointes BM, Bruix M, Thurlkill RL, Schell D, Newsom S, Grimsley GR, Shaw KL, Trevino S, Rico M, Briggs JM, Antosiewicz JM, Scholtz JM, Pace CN. Charge-charge interactions are key determinants of the pK values of ionizable groups in ribonuclease Sa (pI=3.5) and a basic variant (pI=10.2). J Mol Biol. 2003; 325(5):1077–1092. [PubMed: 12527309]
55. Antosiewicz JBJM, Elcock AH, Gilson MK, McCammon JA. Computing the Ionization States of proteins with a Detailed Charge Model. J Comput Chem. 1996; 17:1633–1644.
56. Brooks BRBREOBD, States DJ, Swaminathan S, Karplus M. CHARMM: A program for macromolecular energy minimization, and dynamics calculations. J Comput Chem. 1983; 4:187–195.
57. Madura JDBJM, Wade RC, Davis ME, Luty BA, Ilin A, Antosiewicz J, Gilson MK, Bagheri B, Scott LR, McCammon JA. Electrostatics and diffusion of molecules in solution: simulations with the University of Houston Brownian Dynamics program. Computer Physics Communications. 1995; 91(1–3):57–95.
58. Baker NA, Sept D, Joseph S, Holst MJ, McCammon JA. Electrostatics of nanosystems: application to microtubules and the ribosome. Proc Natl Acad Sci U S A. 2001; 98(18):10037–10041. [PubMed: 11517324]
59. Capriotti E, Fariselli P, Rossi I, Casadio R. A three-state prediction of single point mutations on protein stability changes. BMC Bioinformatics. 2008; 9(Suppl 2):S6.
60. Parthiban V, Gromiha MM, Schomburg D. CUPSAT: prediction of protein stability upon point mutations. Nucleic Acids Res. 2006; 34(Web Server issue):W239–W242. [PubMed: 16845001]

61. Frappier V, Chartier M, Najmanovich RJ. ENCoM server: exploring protein conformational space and the effect of mutations on protein function and stability. Nucleic Acids Res. 2015; 43(W1):W395–W400. [PubMed: 25883149]

62. Frappier V, Najmanovich RJ. A coarse-grained elastic network atom contact model and its use in the simulation of protein dynamics and the prediction of the effect of mutations. PLoS computational biology. 2014; 10(4):e1003569. [PubMed: 24762569]

63. Atilgan AR, Durell SR, Jernigan RL, Demirel MC, Keskin O, Bahar I. Anisotropy of fluctuation dynamics of proteins with an elastic network model. Biophysical journal. 2001; 80(1):505–515. [PubMed: 11159421]

64. Ichiye T, Karplus M. Collective motions in proteins: a covariance analysis of atomic fluctuations in molecular dynamics and normal mode simulations. Proteins. 1991; 11(3):205–217. [PubMed: 1749773]

65. Eyal E, Yang LW, Bahar I. Anisotropic network model: systematic evaluation and a new web interface. Bioinformatics. 2006; 22(21):2619–2627. [PubMed: 16928735]

66. Bakan A, Meireles LM, Bahar I. ProDy: protein dynamics inferred from theory and experiments. Bioinformatics. 2011; 27(11):1575–1577. [PubMed: 21471012]

67. Herrero-Gonzalez, SaDCA. New Routes to Old Places: PIK3R1 and PIK3R2 Join PIK3CA and PTEN as Endometrial Cancer Genes. Cancer Discovery. 2011:106–107. [PubMed: 22586352]

68. Saito M, Okamoto A, Kohno T, Takakura S, Shinozaki H, Isonishi S, Yasuhara T, Yoshimura T, Ohtake Y, Ochiai K, Yokota J, Tanaka T. Allelic imbalance and mutations of the PTEN gene in ovarian cancer. Int J Cancer. 2000; 85(2):160–165. [PubMed: 10629071]

69. Xu B, Hamada S, Kusuki I, Itoh R, Kitawaki J. Possible involvement of loss of heterozygosity in malignant transformation of ovarian endometriosis. Gynecol Oncol. 2011; 120(2):239–246. [PubMed: 21130491]

70. Maehama T, Taylor GS, Dixon JE. PTEN and myotubularin: novel phosphoinositide phosphatases. Annu Rev Biochem. 2001; 70:247–279. [PubMed: 11395408]

71. Minaguchi T, Yoshikawa H, Oda K, Ishino T, Yasugi T, Onda T, Nakagawa S, Matsumoto K, Kawana K, Taketani Y. PTEN mutation located only outside exons 5, 6, and 7 is an independent predictor of favorable survival in endometrial carcinomas. Clin Cancer Res. 2001; 7(9):2636–2642. [PubMed: 11555573]

72. Miller MP, Kumar S. Understanding human disease mutations through the use of interspecific genetic variation. Hum Mol Genet. 2001; 10(21):2319–2328. [PubMed: 11689479]

73. Mooney SD, Klein TE. The functional importance of disease-associated mutation. BMC Bioinformatics. 2002; 3:24. [PubMed: 12220483]

74. Iijima M, Huang YE, Luo HR, Vazquez F, Devreotes PN. Novel mechanism of PTEN regulation by its phosphatidylinositol 4,5-bisphosphate binding motif is critical for chemotaxis. J Biol Chem. 2004; 279(16):16606–16613. [PubMed: 14764604]

75. Zhang XC, Piccini A, Myers MP, Van Aelst L, Tonks NK. Functional analysis of the protein phosphatase activity of PTEN. Biochem J. 2012; 444(3):457–464. [PubMed: 22413754]

76. Chia JY, Gajewski JE, Xiao Y, Zhu HJ, Cheng HC. Unique biochemical properties of the protein tyrosine phosphatase activity of PTEN-demonstration of different active site structural requirements for phosphopeptide and phospholipid phosphatase activities of PTEN. Biochim Biophys Acta. 2010; 1804(9):1785–1795. [PubMed: 20685300]

77. Han SY, Kato H, Kato S, Suzuki T, Shibata H, Ishii S, Shiiba K, Matsuno S, Kanamaru R, Ishioka C. Functional evaluation of PTEN missense mutations using in vitro phosphoinositide phosphatase assay. Cancer Res. 2000; 60(12):3147–3151. [PubMed: 10866302]

78. Waite KA, Eng C. Protean PTEN: form and function. Am J Hum Genet. 2002; 70(4):829–844. [PubMed: 11875759]

79. Rodriguez-Escudero I, Oliver MD, Andres-Pons A, Molina M, Cid VJ, Pulido R. A comprehensive functional analysis of PTEN mutations: implications in tumor- and autism-related syndromes. Hum Mol Genet. 2011; 20(21):4132–4142. [PubMed: 21828076]

80. Worby CA, Dixon JE. Pten. Annu Rev Biochem. 2014; 83:641–669. [PubMed: 24905788]

81. Papa A, Wan L, Bonora M, Salmena L, Song MS, Hobbs RM, Lunardi A, Webster K, Ng C, Newton RH, Knoblauch N, Guarnerio J, Ito K, Turka LA, Beck AH, Pinton P, Bronson RT, Wei W,

Pandolfi PP. Cancer-associated PTEN mutants act in a dominant-negative manner to suppress PTEN protein function. Cell. 2014; 157(3):595–610. [PubMed: 24766807]

82. Hollander MC, Blumenthal GM, Dennis PA. PTEN loss in the continuum of common cancers, rare syndromes and mouse models. Nature reviews Cancer. 2011; 11(4):289–301. [PubMed: 21430697]
83. Ishii N, Maier D, Merlo A, Tada M, Sawamura Y, Diserens AC, Van Meir EG. Frequent co-alterations of TP53, p16/CDKN2A, p14ARF, PTEN tumor suppressor genes in human glioma cell lines. Brain pathology. 1999; 9(3):469–479. [PubMed: 10416987]
84. Zainuddin N, Jaafar H, Isa MN, Abdullah JM. Presence of allelic loss and PTEN mutations in malignant gliomas from Malay patients. The Medical journal of Malaysia. 2004; 59(4):468–479. [PubMed: 15779579]
85. Abdullah JM, Farizan A, Asmarina K, Zainuddin N, Ghazali MM, Jaafar H, Isa MN, Naing NN. Association of loss of heterozygosity and PTEN gene abnormalities with paraclinical, clinical modalities and survival time of glioma patients in Malaysia. Asian J Surg. 2006; 29(4):274–282. [PubMed: 17098662]
86. Johnston SB, Raines RT. Conformational stability and catalytic activity of PTEN variants linked to cancers and autism spectrum disorders. Biochemistry. 2015; 54(7):1576–1582. [PubMed: 25647146]
87. Wang SI, Puc J, Li J, Bruce JN, Cairns P, Sidransky D, Parsons R. Somatic mutations of PTEN in glioblastoma multiforme. Cancer Res. 1997; 57(19):4183–4186. [PubMed: 9331071]
88. Chiariello E, Roz L, Albarosa R, Magnani I, Finocchiaro G. PTEN/MMAC1 mutations in primary glioblastomas and short-term cultures of malignant gliomas. Oncogene. 1998; 16(4):541–545. [PubMed: 9484844]
89. Tunca B, Bekar A, Cecener G, Egeli U, Vatan O, Tolunay S, Kocaeli H, Aksoy K. Impact of novel PTEN mutations in Turkish patients with glioblastoma multiforme. Journal of neuro-oncology. 2007; 82(3):263–269. [PubMed: 17151929]
90. Leslie NR, Longy M. Inherited PTEN mutations and the prediction of phenotype. Seminars in cell & developmental biology. 2016; 52:30–38. [PubMed: 26827793]
91. McConechy MK, Ding J, Senz J, Yang W, Melnyk N, Tone AA, Prentice LM, Wiegand KC, McAlpine JN, Shah SP, Lee CH, Goodfellow PJ, Gilks CB, Huntsman DG. Ovarian and endometrial endometrioid carcinomas have distinct CTNNB1 and PTEN mutation profiles. Mod Pathol. 2014; 27(1):128–134. [PubMed: 23765252]
92. Zhang CL, Tada M, Kobayashi H, Nozaki M, Moriuchi T, Abe H. Detection of PTEN nonsense mutation and psiPTEN expression in central nervous system high-grade astrocytic tumors by a yeast-based stop codon assay. Oncogene. 2000; 19(38):4346–4353. [PubMed: 10980610]
93. Kato H, Kato S, Kumabe T, Sonoda Y, Yoshimoto T, Kato S, Han SY, Suzuki T, Shibata H, Kanamaru R, Ishioka C. Functional evaluation of p53 and PTEN gene mutations in gliomas. Clin Cancer Res. 2000; 6(10):3937–3943. [PubMed: 11051241]
94. Parsons DW, Jones S, Zhang X, Lin JC, Leary RJ, Angenendt P, Mankoo P, Carter H, Siu IM, Gallia GL, Olivi A, McLendon R, Rasheed BA, Keir S, Nikolskaya T, Nikolsky Y, Busam DA, Tekleab H, Diaz LA Jr, Hartigan J, Smith DR, Strausberg RL, Marie SK, Shinjo SM, Yan H, Riggins GJ, Bigner DD, Karchin R, Papadopoulos N, Parmigiani G, Vogelstein B, Velculescu VE, Kinzler KW. An integrated genomic analysis of human glioblastoma multiforme. Science. 2008; 321(5897):1807–1812. [PubMed: 18772396]
95. Chi AS, Batchelor TT, Dias-Santagata D, Borger D, Stiles CD, Wang DL, Curry WT, Wen PY, Ligon KL, Ellisen L, Louis DN, Iafrate AJ. Prospective, high-throughput molecular profiling of human gliomas. Journal of neuro-oncology. 2012; 110(1):89–98. [PubMed: 22821383]
96. Williams G. Elastic network model of allosteric regulation in protein kinase PDK1. BMC Struct Biol. 2010; 10:11. [PubMed: 20500829]
97. Rasheed BK, Stenzel TT, McLendon RE, Parsons R, Friedman AH, Friedman HS, Bigner DD, Bigner SH. PTEN gene mutations are seen in high-grade but not in low-grade gliomas. Cancer Res. 1997; 57(19):4187–4190. [PubMed: 9331072]
98. Duerr EM, Rollbrocker B, Hayashi Y, Peters N, Meyer-Puttlitz B, Louis DN, Schramm J, Wiestler OD, Parsons R, Eng C, von Deimling A. PTEN mutations in gliomas and glioneuronal tumors. Oncogene. 1998; 16(17):2259–2264. [PubMed: 9619835]

99. Bostrom J, Cobbers JM, Wolter M, Tabatabai G, Weber RG, Lichter P, Collins VP, Reifenberger G. Mutation of the PTEN (MMAC1) tumor suppressor gene in a subset of glioblastomas but not in meningiomas with loss of chromosome arm 10q. Cancer Res. 1998; 58(1):29–33. [PubMed: 9426052]

100. Fults D, Pedone CA, Thompson GE, Uchiyama CM, Gumpper KL, Iliev D, Vinson VL, Tavtigian SV, Perry WL 3rd. Microsatellite deletion mapping on chromosome 10q and mutation analysis of MMAC1, FAS, and MXI1 in human glioblastoma multiforme. International journal of oncology. 1998; 12(4):905–910. [PubMed: 9499454]

101. Schmidt EE, Ichimura K, Goike HM, Moshref A, Liu L, Collins VP. Mutational profile of the PTEN gene in primary human astrocytic tumors and cultivated xenografts. Journal of neuropathology and experimental neurology. 1999; 58(11):1170–1183. [PubMed: 10560660]

102. Jeuken JW, Nelen MR, Vermeer H, van Staveren WC, Kremer H, van Overbeeke JJ, Boerman RH. PTEN mutation analysis in two genetic subtypes of high-grade oligodendroglial tumors. PTEN is only occasionally mutated in one of the two genetic subtypes. Cancer genetics and cytogenetics. 2000; 119(1):42–47. [PubMed: 10812170]

103. Tohma Y, Gratas C, Biernat W, Peraud A, Fukuda M, Yonekawa Y, Kleihues P, Ohgaki H. PTEN (MMAC1) mutations are frequent in primary glioblastomas (de novo) but not in secondary glioblastomas. Journal of neuropathology and experimental neurology. 1998; 57(7):684–689. [PubMed: 9690672]

104. Maier D, Zhang Z, Taylor E, Hamou MF, Gratzl O, Van Meir EG, Scott RJ, Merlo A. Somatic deletion mapping on chromosome 10 and sequence analysis of PTEN/MMAC1 point to the 10q25-26 region as the primary target in low-grade and high-grade gliomas. Oncogene. 1998; 16(25):3331–3335. [PubMed: 9681833]

105. Davies MP, Gibbs FE, Halliwell N, Joyce KA, Roebuck MM, Rossi ML, Salisbury J, Sibson DR, Tacconi L, Walker C. Mutation in the PTEN/MMAC1 gene in archival low grade and high grade gliomas. Br J Cancer. 1999; 79(9–10):1542–1548. [PubMed: 10188904]

106. Peraud A, Watanabe K, Schwechheimer K, Yonekawa Y, Kleihues P, Ohgaki H. Genetic profile of the giant cell glioblastoma. Laboratory investigation; a journal of technical methods and pathology. 1999; 79(2):123–129. [PubMed: 10068201]

107. Fulci G, Labuhn M, Maier D, Lachat Y, Hausmann O, Hegi ME, Janzer RC, Merlo A, Van Meir EG. p53 gene mutation and ink4a–arf deletion appear to be two mutually exclusive events in human glioblastoma. Oncogene. 2000; 19(33):3816–3822. [PubMed: 10949938]

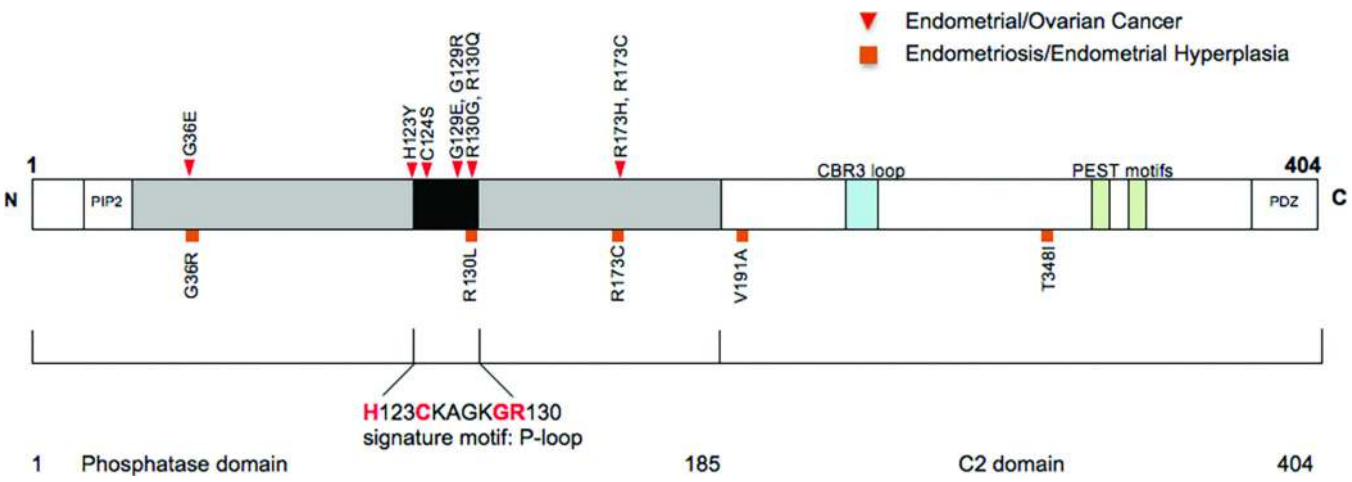

Figure 1. Mutation distribution within the domain structure of human PTEN

The majority of the identified missense mutations found in endometriosis, endometrial and ovarian cancers cluster within the signature motif of the phosphatase domain. Distributions of *PTEN* somatic missense mutations in endometrial and ovarian cancers as well as endometriosis and endometrial hyperplasia are represented by *red* triangles and *orange* squares, respectively. The *grey* and *black* boxes represent the phosphatase domain and the catalytic signature motif, respectively.

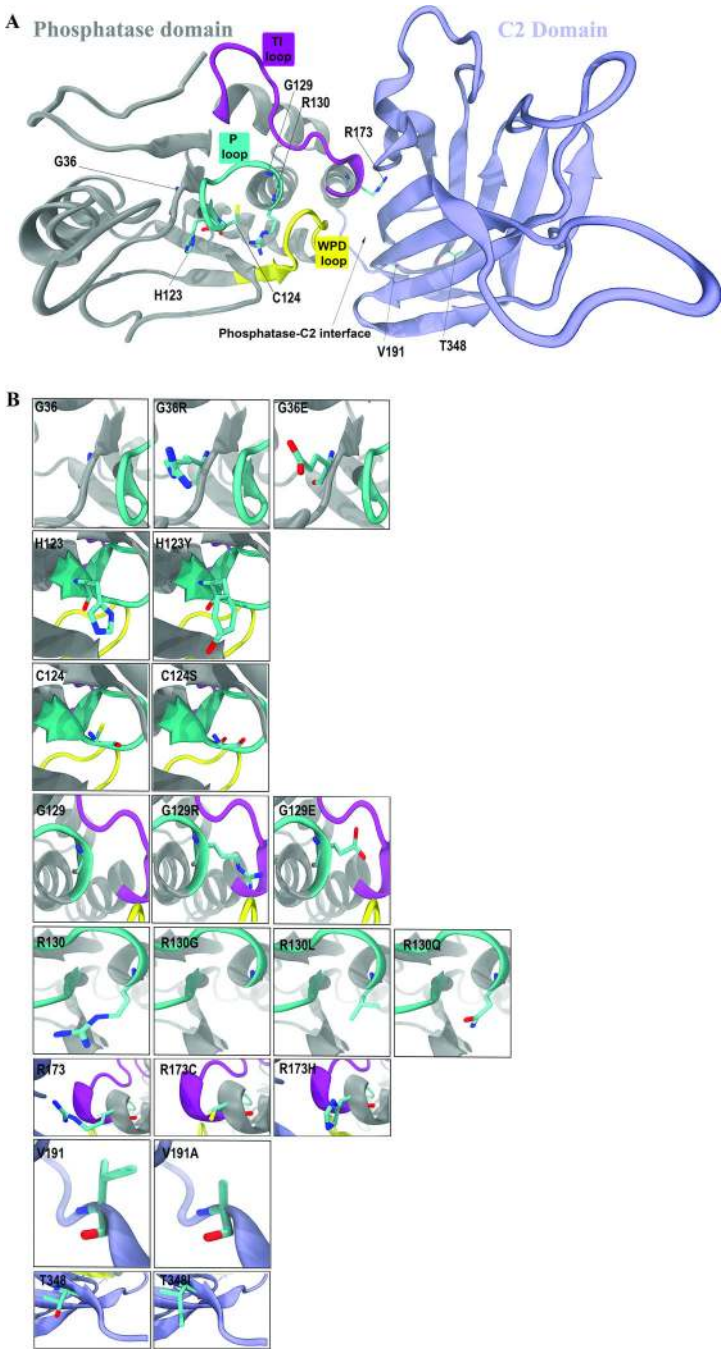

Figure 2. Three-dimensional structure of PTEN and mutants

[A] Phosphatase domain (*grey*) and C2 domain (*purple*) of WT PTEN structure with residues in stick representation. The catalytic P, WPD and TI loops are colored in *cyan, yellow* and *purple* respectively. [B] 13 somatic missense mutations associated with endometriosis, endometrial and ovarian cancers with mutated residues in stick representation.

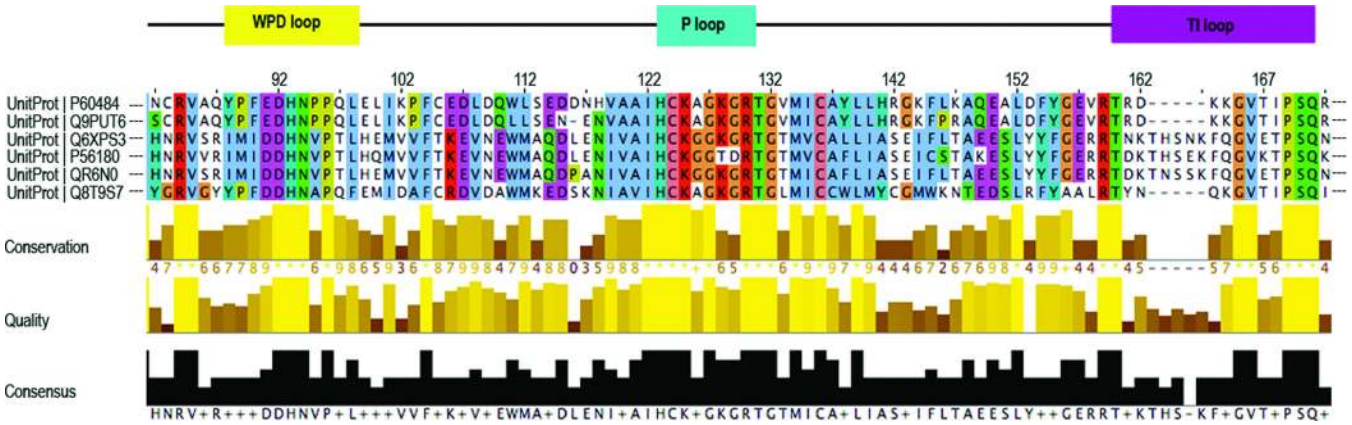

Figure 3. Multiple sequence alignment of PTEN catalytic loops

The region of greatest conservation is the P loop as indicated by '*' and the high conservation scoring. The location of the catalytic WPD, P, and TI loops are indicated above the alignment in *yellow, cyan* and *purple* respectively.

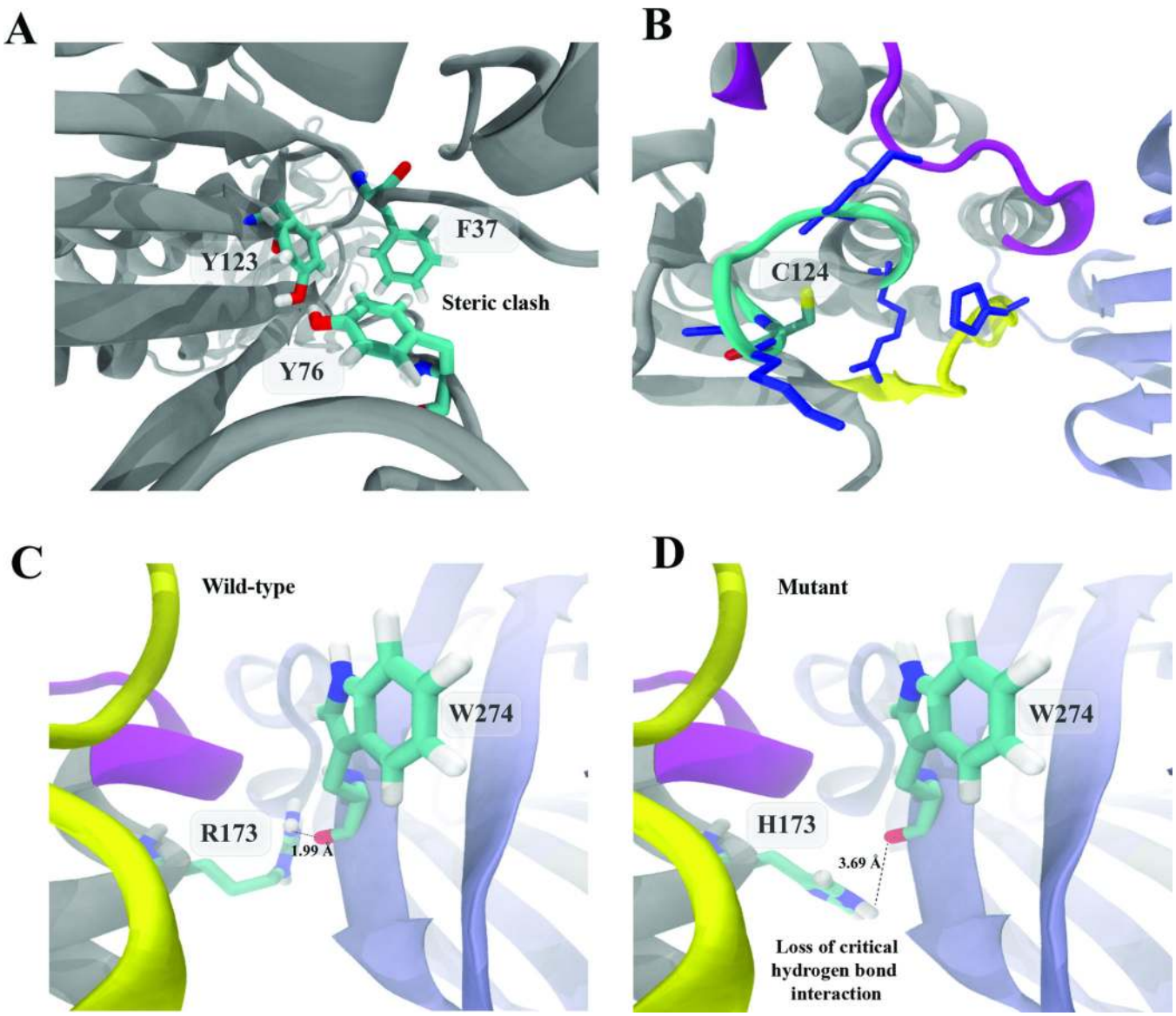

Figure 4. Structural analysis of WT PTEN

[A] H123Y, [B] C124, (basic residues are indicated in *blue*), [C] R173 and [D] H173. Introduction of mutations disturb the structure and disrupt hydrogen bonding. The H123Y mutation causes steric clashing with the neighboring Y76 residue resulting in a distortion of the WPD loop. The high density of basic residues surrounding C124 lowers its pKa (Table 4). The R173H mutation disrupts critical hydrogen bond network interactions within the inter-domain region.

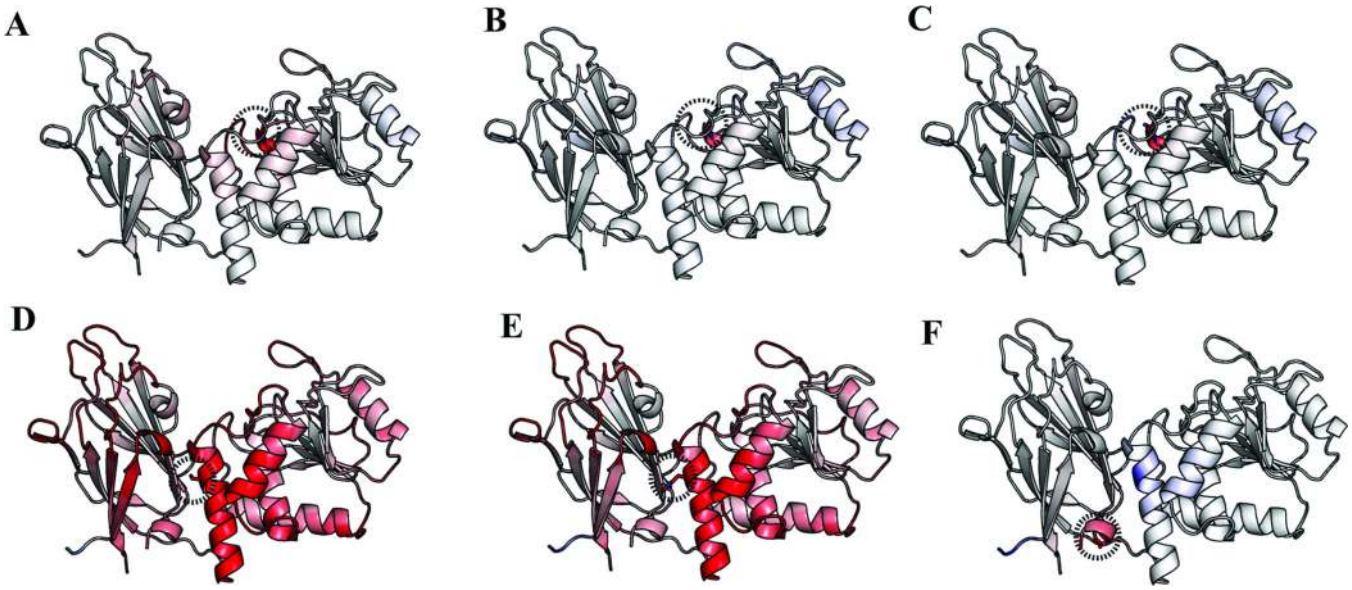

Figure 5. Effect of PTEN mutations on structural stability and dynamics

[A] R130G, [B] R130L, [C] R130Q, [D] R173C, [E] R173H and [F] V191A. Where *black* dotted circle represents the residue mutation and *red* corresponds to an increase in global protein flexibility.

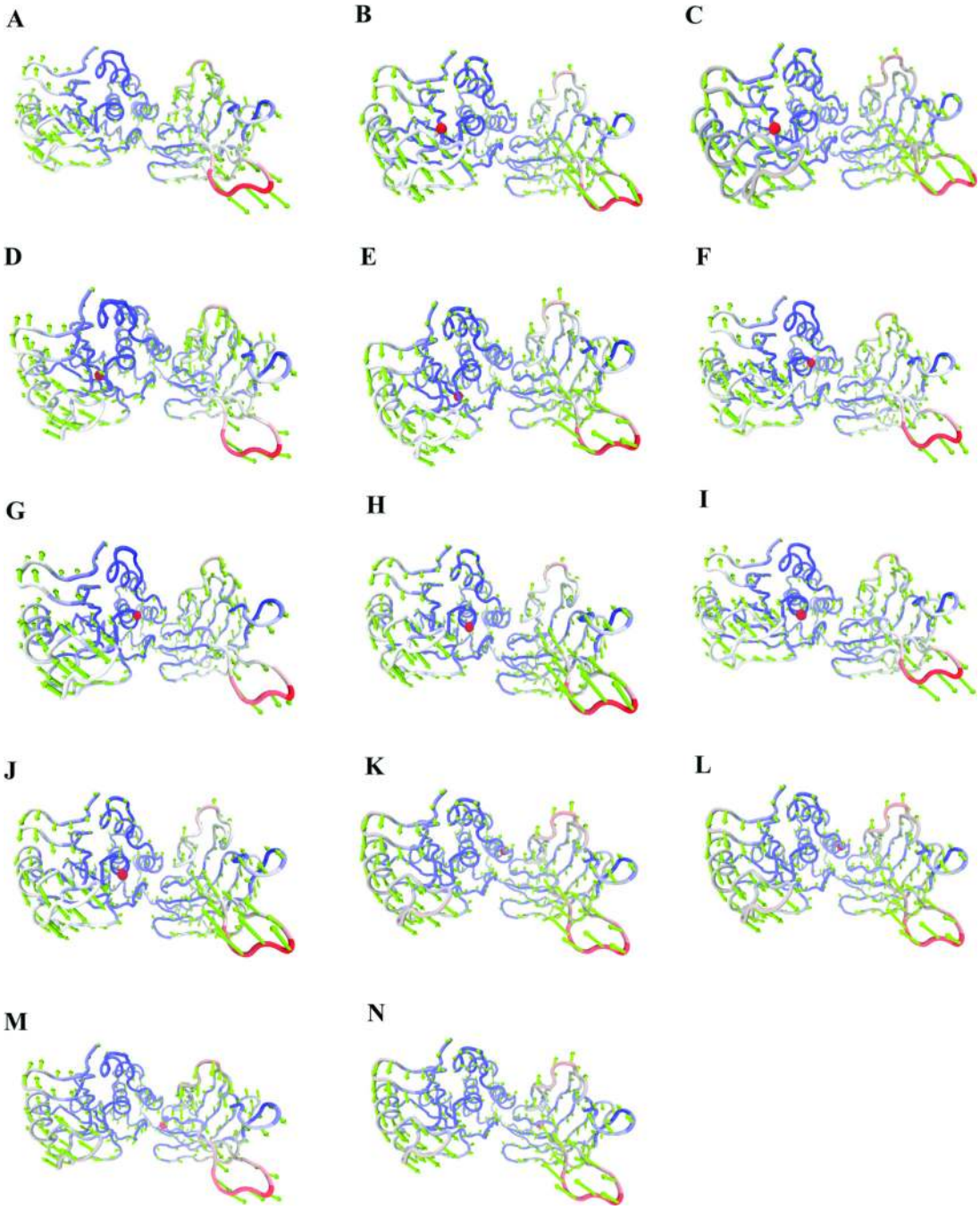

Figure 6. Global motions of WT PTEN and mutants

[A] WT, [B] G36E, [C] G36R, [D] H123Y, [E] C124S, [F] G129E, [G] G129R, [H] R130G, [I] R130L, [J] R130Q, [K] R173C, [L] R173H, [M] V191A, [N] T348I. The magnitude and direction of the displacement for mode 2 of wild-type and PTEN mutants are represented by *green* arrows. The Cα atoms in *red* indicate large global fluctuations, whereas *blue* color corresponds to small global fluctuations. Mutated residues are indicated as *red* spheres.

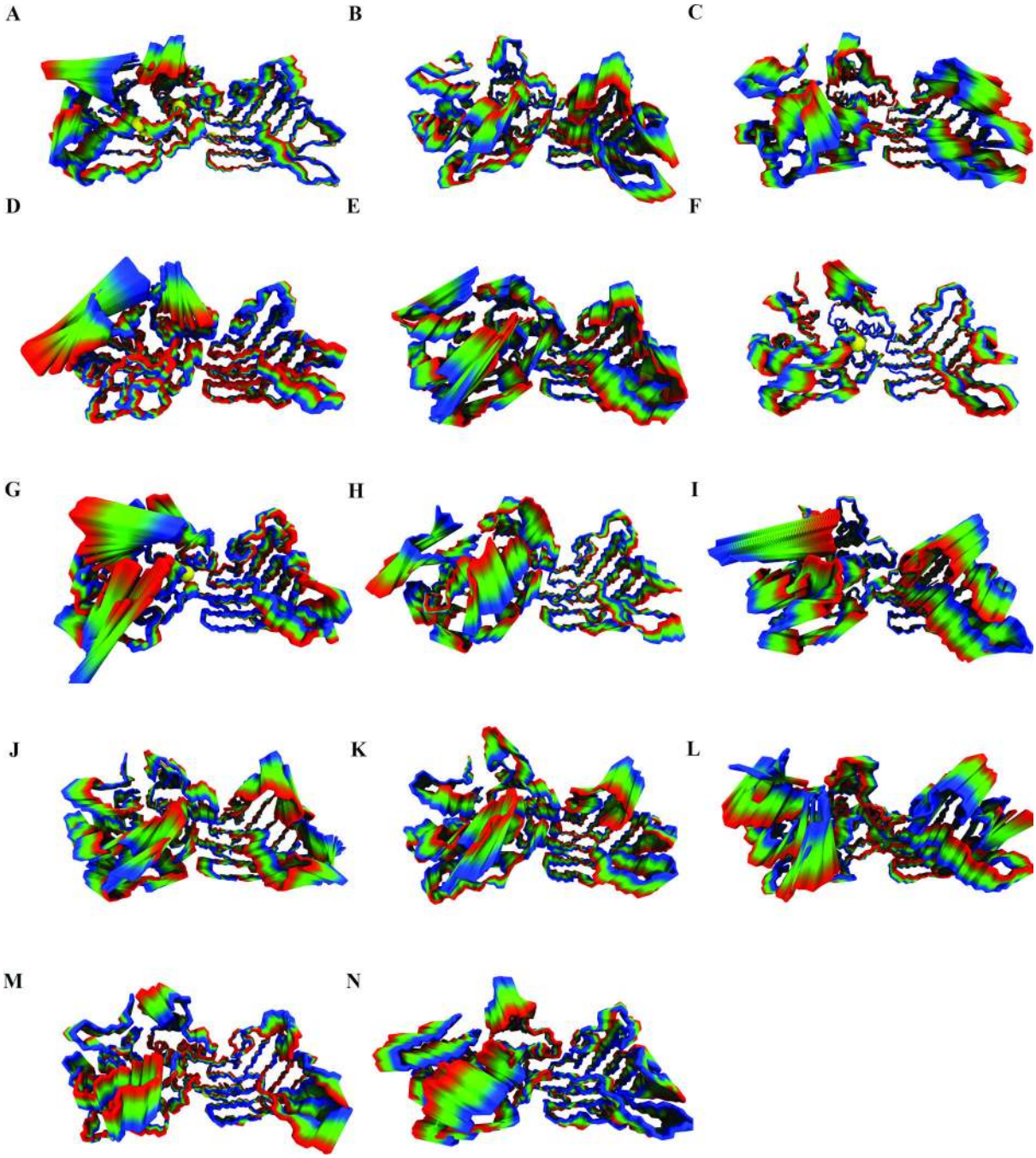

Figure 7. Protein dynamics fingerprint of WT PTEN and mutants

The projections of the displacement described by the first principle component on the structure are shown for [A] WT, [B] G36E, [C] G36R, [D] H123Y, [E] C124S, [F] G129E, [G] G129R, [H] R130G, [I] R130L, [J] R130Q, [K] R173C, [L] R173H, [M] V191A, [N] T348I with 50 frames of the entire trajectory. The structural segments illustrate large concerted motions that bring out the dynamic variations. The protein is represented in the licorice model and colored from *blue* to *red* representing from minimum to maximum motions, respectively. The mutated residue is indicated by a *yellow* sphere.

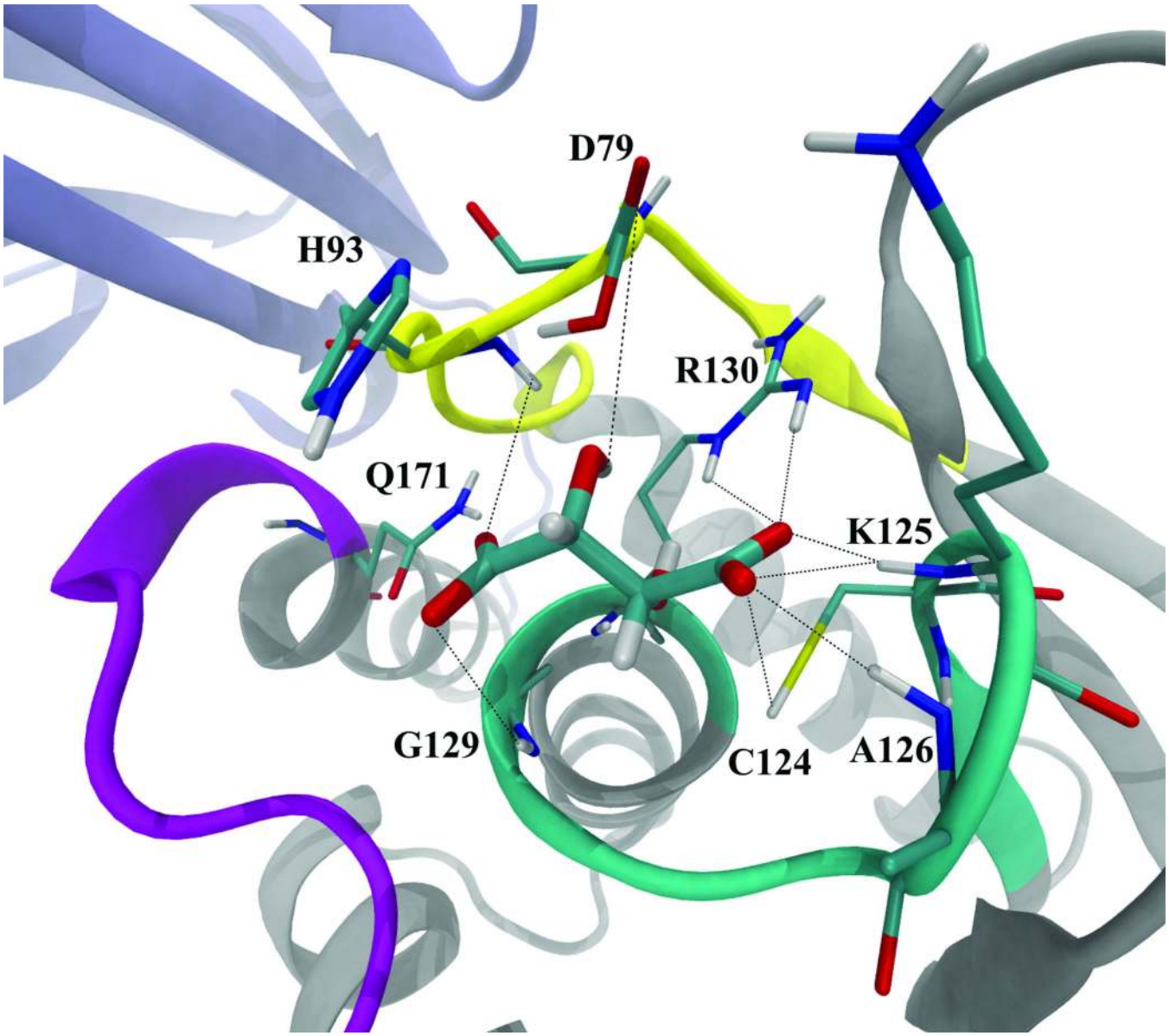

Figure 8. PTEN active site with tartrate molecule

Interactions between tartrate molecule and ionizable residues within the active site.

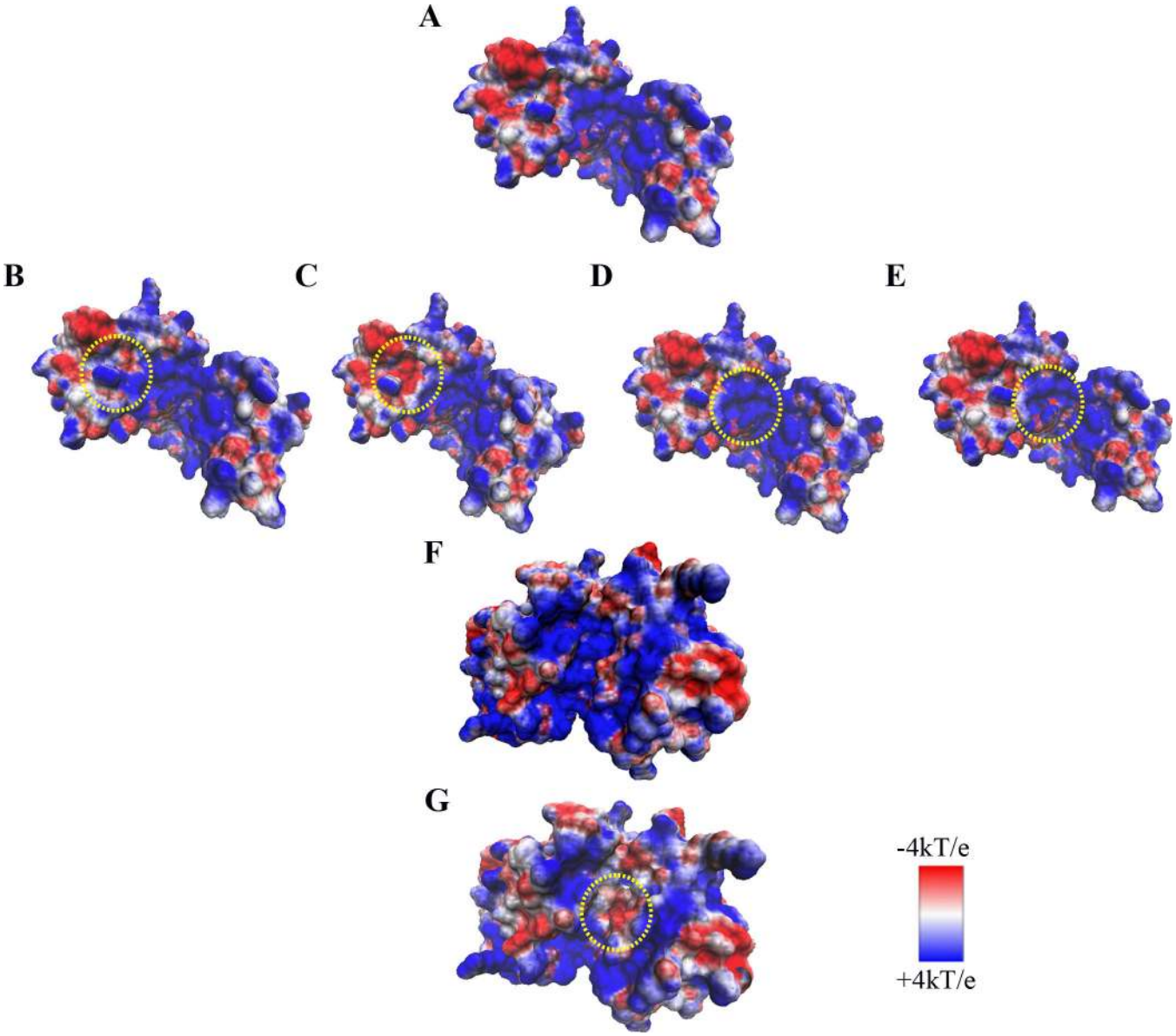

Figure 9. Electrostatic surface potential of WT PTEN and mutants

[A] WT (front-active site), [B] G36R, [C] G36E, [D] G129R, [E] G129E, [F] WT (back) [G] R173C. The mutation sites are indicated with a *yellow* dashed circle illustrating the change in electrostatic potential. The positive potential is colored in *blue* and the negative potential is colored in *red*. Contoured at −4 (*red*) and +4 (*blue*) kcal/mol/electron isovalues.

Table 1

PTEN somatic missense mutations and phenotype

Mutations	Phenotype	Domain	Reference
p.G36R	Endometrial Hyperplasia	Phosphatase	Maxwell et al. 1998; Minaguchi et al. 2001
p.G36E	Endometrial Cancer		Dutt et al. 2008
p.H123Y	Endometrial Cancer		Myers et al. 1997; Bonneau et al. 2000
p.C124S	Endometrial Cancer		Kurose et al. 1998
p.G129R	Endometrial Cancer		Risinger et al. 1997; Furnari et al. 1997
p.G129E	Endometrial Cancer		Risinger et al. 1997; Weng et al. 2001
p.R130G	Endometrial Cancer		Bonneau et al. 2000; Obata et al. 1998; Byron et al. 2008; Dutt et al. 2008; Oda et al. 2005; Minaguchi et al. 2001
	Endometriosis		Willner et al. 2007
	Ovarian Cancer		Lovly et al. 2015
p.R130Q	Ovarian Cancer		Sampson 1925; Sainz de la Cuesta et al. 1996; Saito et al. 2000; Castiblanco et al. 2006; Mandai et al. 2009; Xu et al. 2011 Lovly et al. 2015
p.R130L	Endometriosis		Maxwell et al. 1998; Han et al. 2000; Obata et al. 1998
p.R173C	Endometrial Hyperplasia		Maxwell et al. 1998; Risinger et al. 1998
	Endometrial Cancer		Bussaglia et al. 2000; Minaguchi et al. 2001; Dutt et al. 2008; Risinger et al. 1998
p.R173H	Ovarian Cancer		Sampson 1925; Sainz de la Cuesta et al. 1996; Saito et al. 2000; Castiblanco et al. 2006; Mandai et al. 2009; Xu et al. 2011
p.V191A	Endometrial Hyperplasia	C2	Maxwell et al. 1998; Han et al. 2000
p.T348I	Endometrial Hyperplasia		Maxwell et al. 1998; Georgescu et al. 1999; Han et al. 2000

Table 2

Predicted Effects on Protein Stability (ΔΔG) for the 13 *PTEN* missense mutations

Mutation	I-Mutant 3.0		CUPSAT (thermal)			ENCoM	
	ΔΔG kcal/mol	Predicted Impact	ΔΔG kcal/mol	Predicted Impact	Torsion Angle	ΔΔG kcal/mol	Predicted Impact
p.G36E	−1.30	Destabilizing	+2.04	Stabilizing	Unfavorable	−0.54	Stabilizing
p.G36R	−0.94	Destabilizing	−2.77	Destabilizing	Unfavorable	−0.91	Stabilizing
p.H123Y	−0.67	Destabilizing	−2.13	Destabilizing	Favorable	−0.44	Stabilizing
p.C124S	−1.12	Destabilizing	+3.09	Stabilizing	Unfavorable	−0.17	Stabilizing
p.G129E	−1.33	Destabilizing	−2.30	Destabilizing	Favorable	−0.73	Stabilizing
p.G129R	−1.03	Destabilizing	−2.83	Destabilizing	Favorable	−1.15	Stabilizing
p.R130G	−2.15	Destabilizing	−2.21	Destabilizing	Unfavorable	+1.45	Destabilizing
p.R130L	−0.56	Destabilizing	+0.66	Stabilizing	Favorable	+0.23	Destabilizing
p.R130Q	−1.56	Destabilizing	+0.23	Stabilizing	Favorable	+0.27	Destabilizing
p.R173C	−1.57	Destabilizing	−0.27	Destabilizing	Unfavorable	+0.53	Destabilizing
p.R173H	−1.71	Destabilizing	+0.65	Stabilizing	Unfavorable	+0.12	Destabilizing
p.V191A	−0.18	Destabilizing	−1.39	Destabilizing	Unfavorable	+0.32	Destabilizing
p.T348I	−1.61	Destabilizing	−0.53	Destabilizing	Unfavorable	−0.86	Stabilizing

The results of the structure web-based tools are in kcal/mol and negative (ΔΔG) energy change indicates that the mutation is predicted to destabilize the mutant *PTEN* structure, while positive (ΔΔG) energy suggests stabilization of the structure.

Table 3

WT *PTEN* pKa calculation

Residue	pKa Expected	pKa Observed	pKa Delta
D92	4.00	−2.71	−6.72
H93	6.30	5.93	−0.37
D115	4.00	6.57	2.57
H123	6.30	4.59	−1.71
C124	8.30	3.79	−4.51
K125	10.50	≫pH	≫pH
K128	10.50	8.94	−1.56
R130	12.40	≫pH	≫pH

pKa calculations were performed with wild-type 1D5R structure without substrate. The pKa of the catalytic residue C124 showed a substantial shift toward greater acidity, which is attributable to the surrounding high density of basic residues.